AGU ADVANCING EARTH AND SPACE SCIENCE

Water Resources Research

RESEARCH ARTICLE
10.1029/2022WR032967

Combining Remotely Sensed Evapotranspiration and an Agroecosystem Model to Estimate Center-Pivot Irrigation Water Use at High Spatio-Temporal Resolution

Jingwen Zhang[1,2,3], Kaiyu Guan[2,3,4], Wang Zhou[2,3], Chongya Jiang[2,3], Bin Peng[2,3,4], Ming Pan[5], Robert F. Grant[6], Trenton E. Franz[7], Andrew Suyker[7], Yi Yang[2,3], Xiaohong Chen[1], Kairong Lin[1], and Zewei Ma[2,3]

[1]School of Civil Engineering, Center of Water Resources and Environment, Sun Yat-sen University, Zhuhai, China, [2]Agroecosystem Sustainability Center, Institute for Sustainability, Energy, and Environment, University of Illinois at Urbana Champaign, Urbana, IL, USA, [3]Department of Natural Resources and Environmental Sciences, College of Agricultural, Consumer and Environmental Sciences, University of Illinois at Urbana Champaign, Urbana, IL, USA, [4]National Center for Supercomputing Applications, University of Illinois at Urbana Champaign, Urbana, IL, USA, [5]Center for Western Weather and Water Extremes, Scripps Institution of Oceanography, University of California San Diego, La Jolla, CA, USA, [6]Department of Renewable Resources, University of Alberta, Edmonton, AB, Canada, [7]School of Natural Resources, University of Nebraska-Lincoln, Lincoln, NE, USA

Abstract Estimating irrigation water use accurately is critical for sustainable irrigation and studying terrestrial water cycle in irrigated croplands. However, irrigation is not monitored in most places, and current estimations of irrigation water use has coarse spatial and/or temporal resolutions. This study aims to estimate irrigation water use at the daily and field scale through the proposed model-data fusion framework, which is achieved by particle filtering with two configurations (concurrent, CON, and sequential, SEQ) by assimilating satellite-based evapotranspiration (ET) observations into an advanced agroecosystem model, *ecosys*. Two types of experiments using synthetic and real ET observations were conducted to study the efficacy of the proposed framework for estimating irrigation water use at the irrigated fields in eastern and western Nebraska, United States. The experiments using synthetic ET observations indicated that, for two major sources of uncertainties of ET difference between observations and model simulations, which are bias and noise, noise had larger impacts on degrading the estimation performance of irrigation water use than bias. For the experiments using real ET observations, monthly and annual estimations of irrigation water use matched well with farmer irrigation records, with Pearson correlation coefficient (r) around 0.80 and 0.50, respectively. Although detecting daily irrigation records was very challenging, our method still gave a good performance with RMSE, BIAS, and r around 2.90, 0.03, and 0.4 mm/d, respectively. Our proposed model-data fusion framework for estimating irrigation water use at high spatio-temporal resolution could contribute to regional water management, sustainable irrigation, and better tracking terrestrial water cycle.

Key Points:

- Combining remotely sensed evapotranspiration (ET) and an agroecosystem model is effective to estimate irrigation water use at daily and field scale
- For two sources of ET uncertainties, noise has larger impacts on degrading the estimation performance of irrigation water use than bias
- Remotely sensed ET observations and ET simulations from *ecosys* with high accuracy can improve the estimations of irrigation water use

Supporting Information:

Supporting Information may be found in the online version of this article.

Correspondence to:

J. Zhang and K. Guan,
jingwenz@illinois.edu;
kaiyug@illinois.edu

Citation:

Zhang, J., Guan, K., Zhou, W., Jiang, C., Peng, B., Pan, M., et al. (2023). Combining remotely sensed evapotranspiration and an agroecosystem model to estimate center-pivot irrigation water use at high spatio-temporal resolution. *Water Resources Research*, *59*, e2022WR032967. https://doi.org/10.1029/2022WR032967

Received 8 JUN 2022
Accepted 27 JAN 2023

Author Contributions:

Conceptualization: Jingwen Zhang, Kaiyu Guan, Xiaohong Chen, Kairong Lin
Data curation: Jingwen Zhang, Wang Zhou, Chongya Jiang, Bin Peng, Trenton E. Franz, Andrew Suyker, Yi Yang, Zewei Ma
Formal analysis: Jingwen Zhang
Funding acquisition: Kaiyu Guan, Ming Pan, Trenton E. Franz
Investigation: Jingwen Zhang
Methodology: Jingwen Zhang, Kaiyu Guan, Wang Zhou, Chongya Jiang, Bin Peng, Ming Pan, Robert F. Grant
Project Administration: Jingwen Zhang, Kaiyu Guan

1. Introduction

Irrigation accounts for more than 70% of total water withdrawals from surface and groundwater globally, which is critical for food production in arid and semi-arid regions (McDermid et al., 2021; Wisser et al., 2008). The intensified global warming and population growth require irrigation expansion to relieve water stress and to maintain crop productivity (McDermid et al., 2021; Rosa et al., 2020). Increased irrigation water use demand exacerbates global water scarcity. To accurately quantify irrigation water use is the prerequisite for efficient agricultural water management and for designing effective water policies (Koch et al., 2020; Zaussinger et al., 2019). In addition, as irrigation is one of the direct human alterations of terrestrial water cycle (McDermid et al., 2021), the estimations of irrigation water use could also help for tracking terrestrial water cycle and to investigate its feedback on regional climate (de Rosnay et al., 2003; Haddeland et al., 2006; L. Jiang et al., 2014; Lawston et al., 2015; Ozdogan et al., 2010). However, irrigation is not monitored in most places thus there is great uncertainty about its timing and amount. Current government irrigation data sets are obtained from the statistical surveys/reports and/or some simple estimation methods, such as soil moisture balance models (FAO, 2021) and energy consumption coefficient method for irrigation pumping (Hurr & Litke, 1989). These data sets usually have coarse spatial resolutions and are static for multiple years, such as Food and Agriculture Organization (FAO)'s global irrigation water use data sets at the country level (FAO, 2021) and USGS's state-level irrigation water use data sets updated

Resources: Jingwen Zhang, Kaiyu Guan, Wang Zhou, Chongya Jiang, Ming Pan, Robert F. Grant, Trenton E. Franz, Andrew Suyker, Zewei Ma
Software: Jingwen Zhang, Wang Zhou, Robert F. Grant, Zewei Ma
Supervision: Jingwen Zhang, Kaiyu Guan, Bin Peng, Ming Pan, Xiaohong Chen, Kairong Lin
Validation: Jingwen Zhang
Visualization: Jingwen Zhang
Writing – original draft: Jingwen Zhang
Writing – review & editing: Jingwen Zhang, Kaiyu Guan, Wang Zhou, Chongya Jiang, Bin Peng, Ming Pan, Robert F. Grant, Trenton E. Franz, Andrew Suyker, Yi Yang, Xiaohong Chen, Kairong Lin, Zewei Ma

every 5 yr (USGS, 2018). The lack of irrigation water use data sets at high spatio-temporal resolution hampers efficient regional water management, designing effective water policies, and understanding terrestrial water cycle in irrigated croplands (Koch et al., 2020; Kumar et al., 2015).

Estimations of irrigation water use has received significant attention in recent years (Foster et al., 2014; Haddeland et al., 2006; Jalilvand et al., 2019; Massari et al., 2021; Sun et al., 2017; Vörösmarty & Sahagian, 2000; Wisser et al., 2008). The existing literature on estimating irrigation water use is mainly classified into two categories. The first type is to incorporate some simplified soil/plant-based irrigation rules with predefined thresholds in the process-based models (de Rosnay et al., 2003; Haddeland et al., 2006; Lawston et al., 2015;Nie et al., 2022, 2018; Ozdogan et al., 2010), such as the most widely used maximum allowable depletion (MAD) irrigation scheme with 50% based on soil moisture (Ozdogan et al., 2010). However, irrigation decisions are complicated by many factors, such as farmers' preferences and irrigation infrastructures, thus these frameworks for estimating irrigation water use accompany large uncertainties from farmers' irrigation behavior and process-based models (Foster et al., 2014; Lamb et al., 2021; D. Wang & Cai, 2009).

Second, estimating irrigation water use relies on remote sensing-based soil moisture and/or evapotranspiration (ET) data sets, as irrigation increases soil moisture and ET significantly in the soil-plant-atmosphere-continuum. From the soil moisture perspective, some studies applied data assimilation methods, such as particle batch smoother, for estimating irrigation water use through integrating remotely sensed soil moisture retrievals (such as SMAP) into the process-based models (Abolafia-Rosenzweig et al., 2019; Filippucci et al., 2020; Kumar et al., 2015; Zaussinger et al., 2019). Some studies also used some simple inverted soil water balance models, such as SM2RAIN proposed by Brocca et al. (2013) for rainfall estimation at first and then adapted for quantifying irrigation (Brocca et al., 2018; Jalilvand et al., 2019). However, estimations of irrigation water use based on remotely sensed soil moisture retrievals is strongly connected with the quality of soil moisture data sets as well as some empirical parameters required in the inverted soil water balance models and/or process-based models, such as soil depth and water holding capacity (Jalilvand et al., 2021; Zappa et al., 2022; K. Zhang et al., 2022). Specifically, current satellite-based large-scale soil moisture data sets, which only provide soil moisture information in the shallow soil depth (<0.05 m), are limited by either coarse spatial resolutions (e.g., >10 km in SMOS L3 and SMAP L3 products; Al Bitar et al., 2017; Chan et al., 2016), or coarse temporal resolutions (6–12 days by using Sentinel-1 SAR information in soil moisture retrieval; Das et al., 2019). Some proposed approaches for soil moisture observations with higher spatial and temporal resolution, such as optical approaches based on SWIR and NDVI (Babaeian et al., 2021, 2018; Sadeghi et al., 2017) and estimating soil moisture via assimilating the remote sensing retrievals (thermal infrared, TIR, and synthetic aperture radar, SAR; Lei et al., 2020), could help for estimating irrigation water use at high spatio-temporal resolution.

Estimations of irrigation water use based on remotely sensed ET observations has emerged in recent years. Most studies obtained net ET difference from dual modeling of ET as irrigation water use. Specifically, dual modeling usually used remote sensing-based models (e.g., the two-source energy balance, TSEB, the Priestly-Taylor JPL, PT-JPL, and the Operational Simplified Surface Energy Balance, $SSEB_{op}$) based on surface energy balance with irrigation impact and land surface models (e.g., Noah-MP) and/or hydrological models (e.g., the mesoscale Hydrologic Model, mHM, and World-Wide Water, W3) without irrigation impact (Hain et al., 2015; Koch et al., 2020; Romaguera et al., 2012, 2014; D. Wang & Cai, 2007; C. Zhang & Long, 2021). However, the irrigation water use data sets from these studies usually had coarse temporal (monthly, seasonal, and annual) and/or spatial (1–5 km) resolutions. Some studies estimated irrigation water use through long-term net water balance based on land surface/hydrological models with assimilation of satellite-based information, such as ET, soil moisture, leaf area index (LAI), and land surface temperature (LST; Van Dijk et al., 2018). However, these studies ignored the water unavailable for crop use, such as runoff, drainage, and deep percolation, and also had coarse temporal and/or spatial resolutions. Some researchers estimated irrigation water use using machine learning but required the detailed irrigation water use data sets, such as the in situ pumping records (Wei et al., 2022).

Model-data fusion approaches integrate models and observations to improve the accuracy of model predictions (Gettelman et al., 2022; Y.-P. Wang et al., 2009), which have been applied in many areas, including climate projections using the earth systems (Gettelman et al., 2022), terrestrial carbon cycles tracking (Keenan et al., 2012; Y.-P. Wang et al., 2009), and hydrological cycles simulations (Abrahart & See, 2002; Stampoulis et al., 2019). There are multiple model-data fusion methods, such as data assimilation, Bayesian inference, and model calibration (Gettelman et al., 2022; Guan et al., 2022; Liu & Gupta, 2007; Y.-P. Wang et al., 2009; J. Zhang et al., 2021a). The application of model-data fusion for estimating irrigation water use can be characterized as an inverse

application, analyzing model forcing (i.e., irrigation water use) from observations (e.g., soil moisture and/or ET) with irrigation impacts. This study aims to use the model-data fusion approaches (such as data assimilation) to estimate center-pivot irrigation water use at high spatio-temporal resolution (daily and field scale) based on the process-based model and the remotely sensed ET observations. There are two possible pathways: The first one is to continuously assimilate the remotely sensed ET observations into the process-based models to estimate irrigation timing and amount concurrently. For the second pathway, we assume that the difference between the remotely sensed ET observations with irrigation impacts and ET simulations from *ecosys* without irrigation impacts may reflect the irrigation signals. Thus, the ET difference can be used to check whether irrigation occurs or not (i.e., irrigation timing), and then data assimilation can be applied to determine irrigation amount.

In this study, we proposed a new model-data fusion framework with two configurations, that is, concurrent (CON) and sequential (SEQ), embedded in the particle filtering for estimating center-pivot irrigation water use at high spatio-temporal resolution (daily and field-scale). It was implemented through assimilating remotely sensed ET observations with irrigation impact into the advanced process-based agroecosystem model, *ecosys*. This study aims to address two research questions: (a) What is the efficacy of the new model-data fusion framework for estimating irrigation water use at the daily and field scale? (b) What are the impacts of two major sources (systematic bias and variability, i.e., noise) of uncertainties of ET difference between observations and model simulations on degrading the estimation performance of irrigation water use at high spatio-temporal resolution? To answer these two research questions, two types of experiments using synthetic and real ET observations were conducted at two sets of irrigated fields with center-pivot irrigation systems in eastern and western Nebraska.

2. Methodology

2.1. Model-Data Fusion

The model-data fusion approach integrating a well-calibrated agroecosystem model and remotely sensed ET observations is applied for estimating irrigation water use at high spatio-temporal resolution (daily and field scale, i.e., determined by the field boundary from Common Land Unit, CLU) in this study (Figure 1a). The agroecosystem model is forced with climate and field data, then data assimilation (particle filtering) with two configurations (CONcurrent, CON, and SEQuential, SEQ) is used to update the water fluxes (ET and irrigation) from the agroecosystem model based on the remotely sensed ET observations. Specifically, remotely sensed ET observations with actual irrigation impact are assimilated into the agroecosystem model in real-time at the daily scale through particle filtering to determine when and how much irrigation has already been applied in the past. Irrigation signals are detected from the difference between remotely sensed ET observations with irrigation impact and ET simulations from the agroecosystem model without irrigation impacts.

2.1.1. Concurrent and Sequential Configurations

Two configurations embedded in the data assimilation (particle filtering) for estimating irrigation water use are proposed, including the CONcurrent (CON) and SEQuential (SEQ) (Figures 1b and 1c). CON uses data assimilation for each time period to investigate whether irrigation occurs or not at the daily scale and to estimate corresponding daily irrigation water use amount concurrently (Figure 1b). SEQ first determines whether irrigation occurred or not based on ET difference at the daily scale, and then applies data assimilation at the days with the occurring irrigation to estimate daily irrigation water use amount sequentially (Figure 1c). Specifically, particle filtering is selected as the sequential data assimilation approach. The daily irrigation events are set as the particles in the particle filtering, and they are randomly generated from the random distribution with given irrigation ranges $[0, \beta \times I_{max}]$ mm (β, needs to be calibrated) at the daily scale (Equation 1). If the weight of the irrigation particle with 0 mm amount is maximum among all the particles (irrigation events with different amounts) on the target day, CON claims that there is no irrigation on that day. Otherwise, irrigation occurs on the target day, and the daily irrigation amount is determined as the weighted average of all the irrigation particles. Different from CON, SEQ first determines whether irrigation occurs or not based on the daily relative difference of ET (the ratio of ET difference to ET simulation) on the target day. Specifically, there is no irrigation event on the target day for the case that the daily relative difference of ET between remotely sensed observation with irrigation impact and model simulation without irrigation impact is smaller than the set threshold (α, needs to be calibrated; Equation 2). However, if the daily relative difference of ET reaches the threshold (α), irrigation is assumed as the reason for the large difference of ET. Thus, irrigation occurs on the target day and daily irrigation amount is the weighted average of all the irrigation particles. In addition, estimating irrigation water use is also constrained by the pumping wells and field area (Equation 3).

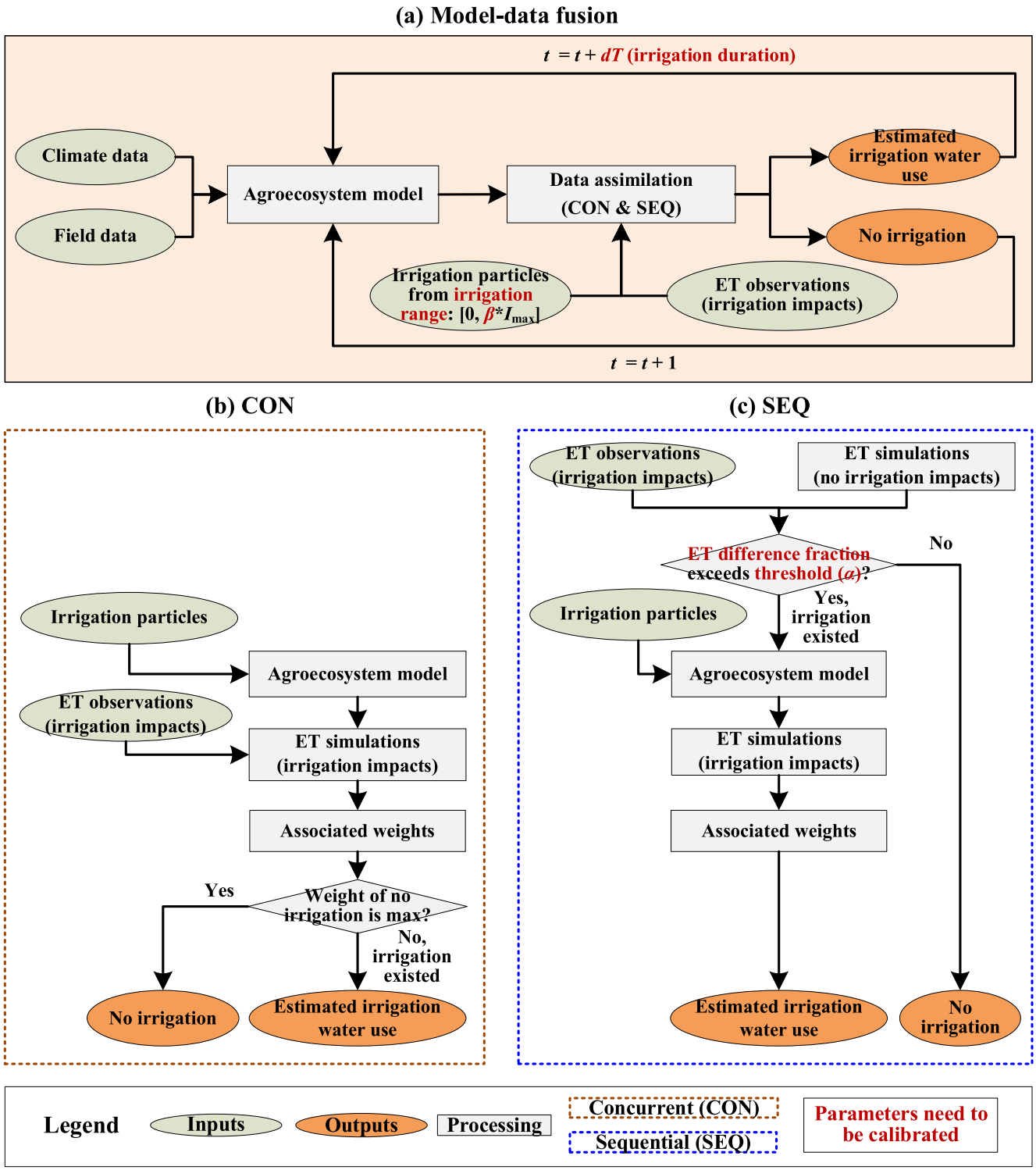

Figure 1. Framework of (a) the proposed model-data fusion approach with two configurations (CON and SEQ) for estimating irrigation water use at high spatio-temporal resolution. (b) Concurrent (CON) determines whether irrigation occurs or not and irrigation water use amount concurrently. (c) Sequential (SEQ) first determines whether irrigation occurred or not and then estimates irrigation water use amount sequentially. Three parameters need to be calibrated for CON and SEQ, including threshold for relative difference of ET (α), irrigation duration (dT), and irrigation range (β).

In addition, once irrigation starts, it usually continues for several days (i.e., irrigation duration, dT, needs to be calibrated). The reason is that center-pivot irrigation systems usually take several days to complete an irrigation cycle due to the large irrigated field, and irrigation will be delayed if a rainfall event exceeds certain amounts during the irrigation cycle, such as the 6.5 mm day^{-1} for 1-day delay, 13 mm day^{-1} for 2-day delay, and 45.5 mm day^{-1} for 7-day delay set in J. Gibson et al. (2017). Thus, irrigation duration (dT) is complicated by multiple factors, such as irrigation systems and climate status.

$$I_t^n \in [0, \beta \times I_{\max}], n = 1, \ldots, N \tag{1}$$

$$\begin{cases} \text{No irrigation,} & \text{if } \dfrac{\left(\mathrm{ET}_{t,obs} - \mathrm{ET}'_{t,sim}\right)}{ET'_{t,sim}} < \alpha \\ \text{Irrigation existing,} & \text{if } \dfrac{\left(\mathrm{ET}_{t,obs} - \mathrm{ET}'_{t,sim}\right)}{\mathrm{ET}'_{t,sim}} \geq \alpha \end{cases} \tag{2}$$

$$I_{\max} = \frac{\text{capacity} \times 24 \times 60 \times 25.4}{S_{\text{field}} \times 27154} \tag{3}$$

where I_t^n is the irrigation particle n at time period t (mm d^{-1}); β is the parameter needed to be calibrated to determine the irrigation ranges to generate all the irrigation particles; N is the particle size; $\mathrm{ET}_{t,obs}$ is the remotely sensed ET observation with irrigation impact at time period t (mm d^{-1}); $\mathrm{ET}'_{t,sim}$ is the model simulation of ET without irrigation impact before data assimilation at time period t (mm d^{-1}); α is the set threshold of the relative difference of ET; and $I_{\max}$ is the maximum allowed irrigation amount (mm d^{-1}), which is usually determined by the capacity of pumping wells of surface water and groundwater for irrigation (gallon per minute, GPM) and the field area (S_{field}, acre) (Equation 3, 1 gallon = 1/27,154 acre-inch, 1 inch = 25.4 mm).

2.1.2. Data Assimilation Through Particle Filtering

Data assimilation, one typical method of model-data fusion, can effectively correct state estimations to reduce uncertainties from process-based models and observations (Moradkhani, 2008; Weerts & El Serafy, 2006; J. Zhang, Cai, et al., 2021). Particle filtering, one of the sequential data assimilation schemes based on Monte Carlo algorithms, is used in this study. The key idea is to determine the final irrigation amount through the weighted average of all the irrigation particles (Weerts & El Serafy, 2006).

Specifically, all the daily irrigation particles are generated from random distribution (Equation 1), then are incorporated into the advanced agroecosystem model to obtain ET simulations with the impacts of different irrigation water use amounts. Note that we combine the uncertainties from the process-based model and observations together, rather than quantifying the ET uncertainties from the process-based model and observations separately. The reason is that the true-values of ET are difficult to obtain without eddy covariance techniques, thus it is difficult to quantify the ET uncertainties from remotely sensed observations. The combined ET uncertainties are represented by the Gaussian distribution (bias, μ_{s-o}, and standard deviation, σ_{s-o}) of ET difference between ET simulations from the calibrated process-based model and remotely sensed ET observations both with irrigation impacts. Then, the probability of all the irrigation particles is determined by the daily ET difference between model simulations with different irrigation particles and remotely sensed observations based on pre-determined Gaussian distribution of ET difference (Equation 4). The ET uncertainties can be reduced through the probability calculation with the pre-determined Gaussian distributions with the parameters (bias, μ_{s-o}, and standard deviation, σ_{s-o}). The associated weights (w_t) for all the irrigation particles are determined as the normalized probabilities (Equation 5).

As irrigation impact is incorporated into the advanced agroecosystem model through the assimilation of remotely sensed ET observations in real-time at the daily scale, the weights of all the particles are determined to be diverse without weight degeneracy. Thus, the resampling scheme is not adopted in this study to simplify its process. Lastly, the final irrigation amount is estimated as the minimum of maximum allowed irrigation amount ($I_{\max}$) and estimations of irrigation water use, which is determined based on the weighted average of all the particles with their associated weights considering the irrigation application efficiency (λ in Equation 6). Note that the irrigation application efficiency of the center pivots is set as 85% to account for the irrigation water loss unavailable for crop use (U.S. GAO, 2019). In general, three parameters (threshold for relative difference of ET, α, irrigation duration, dT, and irrigation range, β) are needed to be calibrated for CON and SEQ.

$$\Delta ET^{n}_{t,sim} = \left(ET^{n}_{t,sim} - ET_{t,obs}\right) \sim N(\mu_{s-o}, \sigma_{s-o}) \tag{4}$$

$$w^{n}_{t} = \frac{pdf\left(\Delta ET^{n}_{t,sim}\right)}{\sum_{n=1}^{N} pdf\left(\Delta ET^{n}_{t,sim}\right)} \tag{5}$$

$$I^{*}_{t} = \min\left(I_{\max}, \frac{\sum_{n=1}^{N}\left(w^{n}_{t} \times I^{n}_{t}\right)}{\lambda}\right) \tag{6}$$

where $\Delta ET^{n}_{t,sim}$ is the difference of ET between ET simulations ($ET^{n}_{t,sim}$, mm d^{-1}) from the process-based model with the impacts of irrigation particle n and remotely sensed ET observation ($ET_{t,obs}$, mm d^{-1}) with actual irrigation impacts at time period t (mm d^{-1}); the ET difference is assumed to follow the Gaussian distribution with the pre-determined parameters of mean (μ_{s-o}) and standard deviation (σ_{s-o}); $pdf\left(\Delta ET^{n}_{t,sim}\right)$ is the probability of ET difference of irrigation particle n at time period t; w^{n}_{t} is the associated weight of the irrigation particle n at time period t; λ is the irrigation application efficiency of the center pivots (set as 85% in this study); I^{*}_{t} is the estimated irrigation amount at time period t (mm d^{-1}).

2.2. The Process-Based Model: *Ecosys*

The *ecosys* model is used in the model-data fusion as the process-based model. *Ecosys* is an advanced agroecosystem model based on biophysical and biochemical mechanisms, and it uses the multi-layered soil-root-canopy system to track the water, energy, carbon, and nutrient cycles at the hourly scale (Grant, 1995, 1997; Grant et al., 1993). More details about the *ecosys* model can be found in Appendix A. We will implement the sensitivity analysis and model calibration for the *ecosys* model before we use it to estimate irrigation water use. Sensitive parameters related to phenology, canopy carbon assimilation, stomatal conductance, and root water uptake of maize and soybean are screened out using the Sobol method. Then, sensitive parameters of maize and soybean are calibrated separately by minimizing the normalized root mean square error (NRMSE) of daily ET and LAI using eddy covariance measurements in eastern Nebraska and satellite-based data sets in western Nebraska (Equation 7). The NRMSE metric is used to avoid the impacts of different magnitudes of ET and LAI. Irrigation impact is considered through incorporating farmer irrigation records and/or the auto-irrigation scheme based on soil moisture. If farmer irrigation records are available at the field level, they can be provided as the forcing in model calibration. Otherwise, the auto-irrigation scheme in the *ecosys* model with the widely used soil-based MAD-50% with a depth of 0.92 m in the top nine soil layers is applied to incorporate irrigation impact in model calibration (i.e., irrigation is triggered to fill current soil moisture to field capacity when MAD increases above the MAD threshold of 0.5; Malejane et al., 2018). Finally, the planting date within the ranges from USDA NASS weekly Crop Progress Reports in western Nebraska is calibrated individually for each site-year to minimize NRMSE of daily ET and LAI.

$$\begin{aligned}\min obj_{\mathrm{NRMSE}} = &\left(\sqrt{\frac{1}{T \times S}\sum_{s=1}^{S}\sum_{t=1}^{T}\left(ET_{s,t,sim} - ET_{s,t,obs}\right)^{2}}/\sigma(ET_{obs})\right) \\ &+ \left(\sqrt{\frac{1}{T \times S}\sum_{s=1}^{S}\sum_{t=1}^{T}\left(LAI_{s,t,sim} - LAI_{s,t,obs}\right)^{2}}/\sigma(LAI_{obs})\right)\end{aligned} \tag{7}$$

where $ET_{t,sim}$ and $ET_{t,obs}$ represent ET of model simulation and observation at time period t (mm d^{-1}); $LAI_{t,sim}$ and $LAI_{t,obs}$ represent LAI of model simulation and observation at time period t (m^2 m^{-2}); $\sigma(ET_{obs})$ and $\sigma(LAI_{obs})$ are the standard deviations of observed ET and LAI; T and S are the total number of days and irrigated fields, respectively.

2.3. Experimental Design

Two types of experiments are designed in this study, including synthetic and real experiments using synthetic and real ET observations, respectively. The first type of experiments (i.e., synthetic experiments) use the synthetic ET

observations to quantify the impacts of different magnitude of ET uncertainties on the estimation performance of irrigation water use. The performance of estimating irrigation water use through the proposed model-data fusion framework is degraded by the uncertainties of ET difference between observations and simulations from process-based models, which are systematic bias and variability (i.e., standard deviation, treated as noise). The synthetic ET observations are generated by adding random synthetic perturbations (ET_{pert}) to ET simulations from the process-based model with synthetic irrigation records. The perturbations can be attributed to the uncertainties of ET difference between observations and model simulations both with irrigation impact. Thus, three groups of scenarios (including *B*, *V*, and *BV*) are applied to investigate the impacts on degrading the estimation performance of irrigation water use resulting from bias, variability, and the combinations of bias and variability, separately. The first group of six scenarios (B_1, B_2, B_3, B_4, B_5, and B_6) are designed with ET perturbations resulting from different magnitudes of bias (1%, 10%, 20%, 30%, 40%, and 50% of ET observations) but no noise. The second group of six scenarios (V_1, V_2, V_3, V_4, V_5, and V_6) are designed with ET perturbations resulting from different magnitudes of variability (1%, 10%, 20%, 30%, 40%, and 50% of ET observations) but no bias. The third group of six scenarios (BV_1, BV_2, BV_3, BV_4, BV_5, and BV_6) are designed with ET perturbations resulting from different combinations of bias and noise (*VB*1: bias 1% and noise 1%; *VB*2: bias 10% and noise 10%; *VB*3: bias 10% and noise 30%; *VB*4: bias 30% and noise 10%; *VB*5: bias 30% and noise 30%; and *VB*6: bias 50% and noise 50% of ET observations).

The second type of experiments (i.e., real experiments) are the real cases for estimating irrigation water use using real ET observations. Ten replicates of real experiments are applied for each site-year to investigate the robustness of the proposed model-data fusion framework for estimating irrigation water use. Irrigation season for each site-year is determined as the period from the first irrigation day to the last irrigation day based on farmer irrigation records in this study.

Three statistical indexes between estimations of irrigation water use and farmer irrigation records are calculated for each site-year at different temporal scales (daily, weekly, and monthly) for two types of experiments using synthetic and real ET observations, including Pearson correlation coefficient (*r*, Equation 8), root mean square error (RMSE, Equation 9), and BIAS (Equation 10).

$$r = \frac{\sum_{t=1}^{T}\left(I_t^* - \overline{I^*}\right)\left(I_t - \overline{I}\right)}{\sqrt{\sum_{t=1}^{T}\left(I_t^* - \overline{I^*}\right)^2 \sum_{t=1}^{T}\left(I_t - \overline{I}\right)^2}} \tag{8}$$

$$\mathrm{RMSE} = \sqrt{\sum_{t=1}^{T}\frac{\left(I_t^* - I_t\right)^2}{T}} \tag{9}$$

$$\mathrm{BIAS} = \frac{\sum_{t=1}^{T}\left(I_t - I_t^*\right)}{T} \tag{10}$$

where I_t^* is the final estimated irrigation amount at time period *t* (mm d^{-1}); I_t is the irrigation amount based on farmer irrigation records at time period *t* (mm d^{-1}); $\overline{I^*}$ and $\overline{I}$ are the averages of estimations of irrigation water use and farmer irrigation records, respectively; *T* is the total time periods with the unit of day, week, and month.

3. Study Area and Data Sets

3.1. Study Area

Two sets of irrigated fields in eastern and western Nebraska, one of the largest irrigated states in the U.S., were selected for this study (Figure 2a). The first set of irrigated fields in eastern Nebraska were two AmeriFlux sites (US-Ne1 and US-Ne2, https://ameriflux.lbl.gov/) with center pivot irrigation systems, which were located at the University of Nebraska-Lincoln's (UNL) Eastern Nebraska Research and Education Center (ENREC) with annual precipitation around 700–800 mm (Figure 2b). US-Ne1 had continuous maize cropping systems, while US-Ne2 had maize-soybean rotation cropping systems. The second set of irrigated fields were 29 fields located

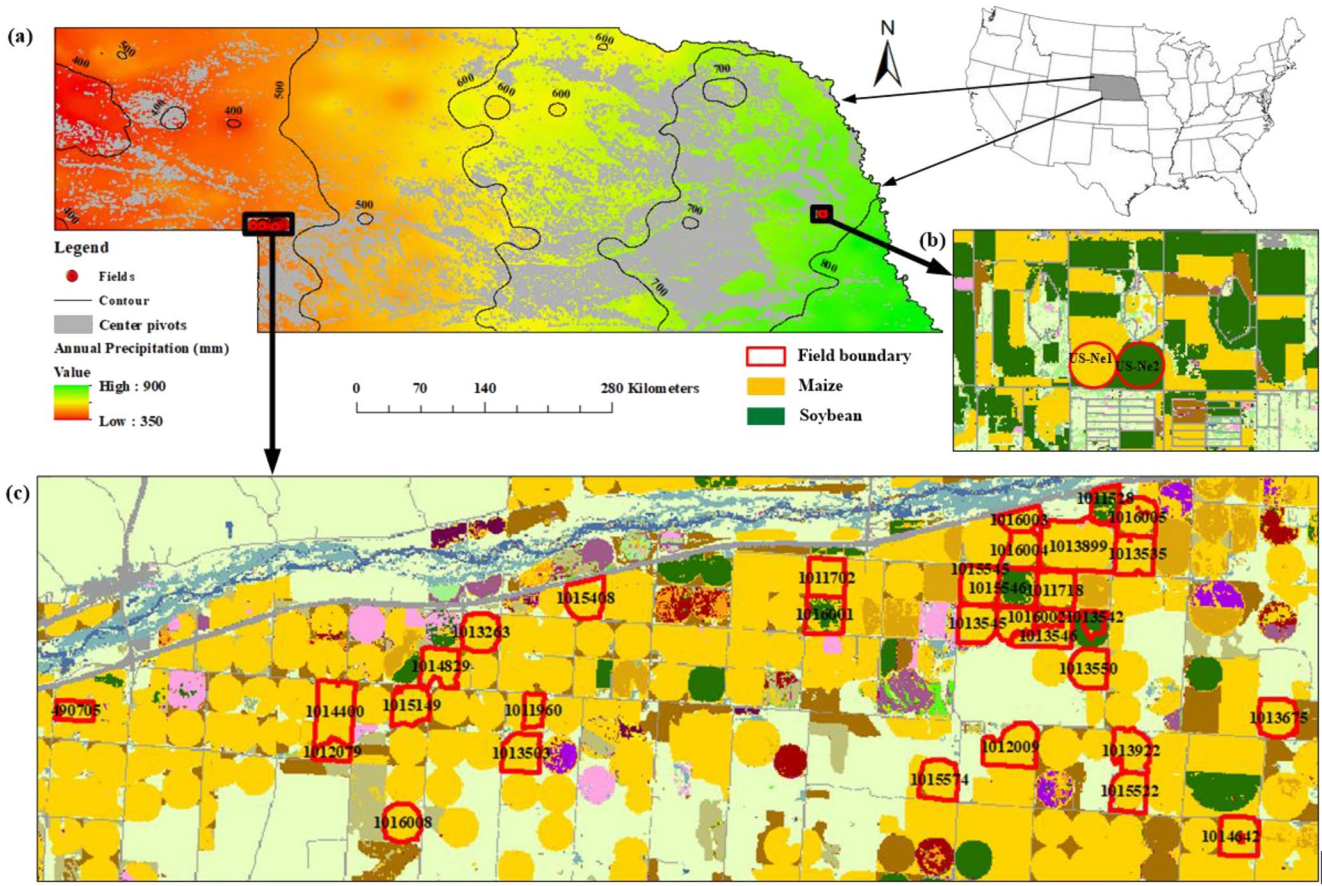

Figure 2. Spatial distribution of two sets of irrigated fields in Nebraska. (a) Location of two sets of irrigated fields with dramatic precipitation difference in Nebraska with the spatial distribution of center pivot irrigation systems (http://snr.unl.edu/data/geographygis/water.aspx). (b) Field boundary of two irrigated fields (US-Ne1 and US-Ne2) with Cropland Data Layer (CDL) in 2002 in eastern Nebraska (annual precipitation around 700–800 mm). (c) Field boundary of 29 irrigated fields with CDL in 2016 in western Nebraska (annual precipitation around 400–500 mm). For the name of each field, the last four digits denote the numbers of irrigated fields, while the remaining digits denote the County FIPS Codes. The numbers 101 and 49 represent Keith and Deuel counties in Nebraska, respectively. The field boundary data was obtained from Common Land Unit, United States Department of Agriculture.

in Keith and Deuel counties in western Nebraska, planted with maize or soybean with annual precipitation around 400–500 mm (Figure 2c and Table S1 in Supporting Information S1).

3.2. Data Sets

3.2.1. Satellite-Based ET and LAI Data Sets

BESS-STAIR ET and LAI data sets at high spatial (30 m) and temporal (daily) resolutions (C. Jiang et al., 2020) during the growing seasons (May–October) in 2015–2016 were used as the satellite-based ET and LAI observations for the second set of irrigated fields in western Nebraska (Table 1). The grid-scale (30 m) ET and LAI data sets were further processed into the field-scale ET and LAI data sets based on the averages of all grids within the field boundary from CLU. Breathing Earth System Simulator (BESS) is a satellite-driven biophysical model, coupling atmosphere and canopy radiative transfer, canopy photosynthesis, and evapotranspiration processes for water, energy, and carbon cycles (C. Jiang & Ryu, 2016). The satellite fusion algorithm, SaTellite dAta IntegRation (STAIR), integrated Landsat data sets with high spatial resolution and MODIS data sets with high temporal resolution to generate daily 30 m resolution surface spectral reflectance under all-sky conditions (Luo et al., 2018, 2020). The daily 30 m surface spectral reflectance data was used to drive the BESS model to generate BESS-STAIR ET and LAI data sets at high spatio-temporal resolution (30 m and daily; C. Jiang et al., 2020). Its satisfactory performance has been demonstrated by benchmarking with 12 eddy covariance sites across the U.S. Corn Belt and by constraining process-based models (such as Noah-MP) on croplands (C. Jiang et al., 2020; Yang et al., 2020).

Table 1
The Details of Data Sets Used for Estimating Irrigation Water Use in Two Types of Experiments at Two Sets of Irrigated Fields in Eastern and Western Nebraska

Experiments type	Location of irrigated fields (time period)	Data sets		Sources
Real experiments using real ET observations	Eastern Nebraska (2001–2012)	ET		AmeriFlux
		LAI		UNL-ENREC's CSP
		Irrigation records (season: start/end date)		UNL-ENREC's CSP
		Meteorological data		AmeriFlux
		Management data (crop type, planting/harvest date, planting density, fertilization records)		UNL-ENREC's CSP
		Soil properties		gSSURGO data sets
	Western Nebraska (2015–2016)	ET		BESS-STAIR data sets
		LAI		STAIR data sets
		Irrigation records (season: start/end date)		AgSense and FieldNET (irrigation software)
		Meteorological data		NLDAS-2
		Field boundary		Common Land Unit (CLU)
		Management data	Crop type	Cropland Data Layer (CDL)
			Planting date	Initial: USDA NASS weekly Crop Progress Reports; final: calibrated
			Harvest date, planting density, fertilization records, tillage practice	Harvested on October 31; planting density (maize: 8.4 plants m^{-2}; soybean: 37.1 plants m^{-2}); fertilizer: 18 g N m^{-2} and 5 g P m^{-2} yr^{-1} applied 2 days before planting; no tillage
		Soil properties		gSSURGO data sets
Synthetic experiments using synthetic ET observations and synthetic irrigation records	Eastern Nebraska (2001–2012)	Synthetic ET observations		Simulations from the *ecosys* model added with perturbations resulting from systematic bias and variability (check Section 3.2.3 for more details)
		Synthetic irrigation records (season: start/end date)		Carbon Sequestration Program (CSP)
		Meteorological, management, and soil data		Same as real experiments in eastern Nebraska

3.2.2. Farmer Irrigation Records at the Field Level

Daily farmer irrigation records at the first set of irrigated fields (two eddy-covariance sites: US-Ne1 and US-Ne2) during the period 2001–2012 were obtained from the Carbon Sequestration Program (CSP) at the UNL ENREC near Mead, Nebraska (http://csp.unl.edu/Public/sites.htm; Table 1). For the second set of irrigated fields in western Nebraska, daily farmer irrigation records during the period from 2015 to 2016 were processed based on the hourly raw data downloaded from AgSense and FieldNET irrigation software provided by the Nebraska Chapter of The Nature Conservancy through the Western Nebraska Irrigation Project (Table 1). The spatially distributed maps of annual and field-scale irrigation water use at the second set of irrigated fields in western Nebraska during the period from 2015 to 2016 were shown in Figure S1 in Supporting Information S1.

3.2.3. Synthetic ET Observations and Irrigation Records

Synthetic ET observations for synthetic experiments (Section 2.3) were generated by adding random synthetic perturbations (ET_{pert}) to ET simulations from the *ecosys* model with synthetic irrigation records (Table 1). ET perturbations (ET_{pert}) resulting from different magnitudes of bias (1%–50% of ET observations) were generated for the first group of six scenarios (B_1, B_2, B_3, B_4, B_5, and B_6 in Equation 11). ET perturbations (ET_{pert}) resulting from different magnitudes of variability (i.e., standard deviation, treated as noise, 1%–50% of ET observations) were generated for the second group of six scenarios (V_1, V_2, V_3, V_4, V_5, and V_6 in Equation 12). ET perturbations (ET_{pert}) resulting from different combinations of bias and noise were generated for the third group of six scenarios (BV_1, BV_2, BV_3, BV_4, BV_5, and BV_6 in Equation 13), including scenarios for both small bias and noise, small bias but large noise, large bias but small noise, and both large bias and noise. ET simulations from *ecosys* have already incorporated irrigation impact through farmer irrigation records, which were treated as synthetic irrigation records. Farmer irrigation records for the irrigated fields in eastern Nebraska were obtained from UNL-ENREC's CSP (Table 1).

$$B_1,\ldots,B_k,\ldots,B_6 : \mathrm{ET}_{t.pert} = \gamma_k \times \mathrm{ET}_{t.obs}, \gamma_k \in [1\%, 10\%, 20\%, 30\%, 40\%, 50\%] \tag{11}$$

$$V_1,\ldots,V_k,\ldots,V_6 : \mathrm{ET}_{t.pert} \sim N(0, \varepsilon_k \times \mathrm{ET}_{t.obs}), \varepsilon_k \in [1\%, 10\%, 20\%, 30\%, 40\%, 50\%] \tag{12}$$

$$BV_1,\ldots,BV_k,\ldots,BV_6 : \mathrm{ET}_{t.pert} \sim N(\gamma_k \times \mathrm{ET}_{t.obs}, \varepsilon_k \times \mathrm{ET}_{t.obs})$$

$$(\gamma_k, \varepsilon_k) \in [(1\%, 1\%); (10\%, 10\%); (10\%, 30\%); (30\%, 10\%); (30\%, 30\%); (50\%, 50\%)] \tag{13}$$

where $ET_{t,pert}$ denoted ET perturbation at time period t (mm d^{-1}), which represented the difference between ET observations and simulations from process-based models both with irrigation impact; B_k represented the kth scenario of the first group of synthetic experiments to investigate the impacts of bias on degrading the estimation performance of irrigation water use; V_k represented the kth scenario of the second group of synthetic experiments to investigate the impacts of variability (noise) on degrading the estimation performance of irrigation water use; BV_k represented the kth scenario of the third group of synthetic experiments to investigate the impacts of the combination of bias and variability (noise) on degrading the estimation performance of irrigation water use; γ_k represented the ratio of ET observations for bias for the kth scenario; and ε_k represented the ratio of ET observations for variability (noise) for the kth scenario.

3.2.4. Other Ancillary Data

The first set of irrigated fields (US-Ne1 and US-Ne2) in Mead, eastern Nebraska had the complete data sets from AmeriFlux during the period 2001–2012, including water (ET), energy (sensible and latent heat), and carbon (gross primary production-GPP and net ecosystem exchange-NEE) fluxes and hourly gap-filled meteorological data (i.e., humidity, downward shortwave radiation, precipitation, air temperature, and wind speed; Table 1). The golden standard data sets of field management and crop growth data, including planting/harvest dates, planting density, fertilization records, and LAI, were obtained from UNL-ENREC's CSP (http://csp.unl.edu/Public/sites.htm).

For the second set of irrigated fields in western Nebraska, the hourly meteorological data (i.e., humidity, downward shortwave radiation, precipitation, air temperature, and wind speed) was obtained from North American Land Data Assimilation System (NLDAS-2). BESS-STAIR ET and LAI data sets were processed into the daily and field-scale ET and LAI observations, while detailed field management and other crop growth data were unavailable. Crop type and field boundary were obtained from Cropland Data Layer and CLU, respectively. The initial planting date of the second set of irrigated fields was obtained from USDA NASS weekly Crop Progress Reports, and crops were harvested on October 31. For fertilizer, 18g N m^{-2} and 5g P m^{-2} per year were applied 2 days before planting for corn while no fertilizer was applied for soybean. Other land management practices were set as the same across all the irrigated fields in western Nebraska, including tillage practice (no-tillage) and planting density (8.4 plants m^{-2} for corn and 37.1 plants m^{-2} for soybean). In addition, soil properties (field capacity, wilting point, saturated hydraulic conductivity, etc) at two sets of irrigated fields in eastern and western Nebraska with a maximum root-zone depth of 2.0 m were obtained from the gSSURGO data set (Table 1).

4. Results

4.1. *Ecosys* Model Performance

The sensitive parameters of the *ecosys* model for maize and soybean were screened out using the Sobol method, respectively (Figures S2 and S3 in Supporting Information S1). The identified sensitive parameters of the *ecosys* model for maize and soybean were then calibrated separately in eastern and western Nebraska. For the irrigated AmeriFlux fields (US-Ne1 and US-Ne2) in eastern Nebraska with detailed ground-based management data, the daily and monthly *ecosys*-simulated ET and LAI of maize and soybean matched very well with the eddy-covariance and ground-based observations (Figures 3a–3d and Figures S4a–S4d in Supporting Information S1). Both R^2 of daily ET of maize and soybean were 0.87, and R^2 of monthly ET of maize and soybean were 0.94 and 0.96, respectively. For LAI, R^2 of maize and soybean at the daily scale were 0.81 and 0.75, respectively; and R^2 of maize and soybean at the monthly scale were 0.83 and 0.91, respectively. *Ecosys* could also capture the magnitude and seasonal patterns of ET and LAI with high accuracy at US-Ne1 and US-Ne2 (Figure S5 in Supporting Information S1). However, as there were no available ground-based management observations at the 29 irrigated fields in western Nebraska, the planting date for each site-year was calibrated using daily and field-scale satellite-based ET and LAI data sets (Table S1 in Supporting Information S1). The scatter of daily and monthly *ecosys*-simulated ET and LAI with the satellite-based observations distributed evenly on both sides of the 1-to-1 line at the field level (Figures 3e–3h and Figures S4e–S4h in Supporting Information S1). R^2 of daily ET of maize and soybean were 0.49 and 0.47, respectively, and R^2 of monthly ET of maize and soybean were 0.91 and 0.85, respectively. For LAI, R^2 of maize and soybean at the daily scale were 0.93 and 0.80, respectively; and R^2 of maize and soybean at the monthly scale were 0.94 and 0.83, respectively.

4.2. Experiments With Synthetic ET Observations

The first type of synthetic experiments (including three groups of scenarios *B*, *V*, and *BV*, more details in Section 2.3) using synthetic ET observations (details in Section 3.2.3) for estimating irrigation water use were conducted at two AmeriFlux fields (US-Ne1 and US-Ne2) in eastern Nebraska during the period from 2001 to 2012. Synthetic ET observations for three groups of scenarios were generated by adding random synthetic perturbations (ET_{pert}) resulting from bias (scenarios *B*), noise (scenarios *V*), and the combination of bias and noise (scenarios *BV*) to virtual observations, that is, ET simulations from *ecosys* with synthetic irrigation records (details in Section 3.2.3). Based on the performance comparison among different particle sizes (8, 10, 20, 30, and 40), we chose the particle size ($N = 10$) in this study via the tradeoff between performance and computation time. Three parameters (threshold for relative difference of ET, α, irrigation range, β, and irrigation duration, dT) of the proposed model-data fusion with CON and SEQ configurations were calibrated manually as 0.02, 3.0, and 1.0, respectively.

Three indexes (*r*, RMSE, and BIAS) between estimations of irrigation water use and synthetic irrigation records at daily, weekly, and monthly scales under three groups of scenarios (*B*, *V*, and *BV*) were summarized in the boxplots (Figures 4 and 5, and Figure S6 in Supporting Information S1). Results indicated that the perturbations resulting from noise had larger impacts on degrading the estimation performance of irrigation water use than those resulting from bias. Pearson correlation coefficients (*r*) of scenarios *V* (perturbations resulting from noise) were lower than those of scenarios *B* (perturbations resulting from bias; Figure 4). For scenarios *BV*, *r* of scenarios BV_2 and BV_4 with smaller noise (10%) were higher than those of scenarios BV_3 and BV_5 with larger noise (30%). In addition, *r* decreased with the perturbations resulting from noise (scenarios *V*), while there was little difference for scenarios *B* with different magnitudes of perturbations resulting from bias. The reason was that bias correction embedded in particle filtering (Equation 4) could effectively remove the impacts of perturbations resulting from bias. For another two indexes (RMSE and BIAS), the similar patterns also were indicated by the results in Figure 5 and Figure S6 in Supporting Information S1. RMSE and BIAS of scenarios *V* (perturbations resulting from noise) were larger than those of scenarios *B* (perturbations resulting from bias). For scenarios *BV*, RMSE and BIAS of scenarios BV_2 (bias: 10%, noise: 10%) and BV_4 (bias: 30%, noise: 10%) were lower than those of scenarios BV_3 (bias: 10%, noise: 30%) and BV_5 (bias: 30%, noise: 30%), which had larger noise but same bias. In addition, RMSE and BIAS increased with the perturbations resulting from noise (scenarios *V*), while there was little difference for scenarios *B* with different magnitudes of perturbations resulting from bias. For the performance at different temporal scales, the statistical indexes (*r* and RMSE) between estimations of irrigation water use and farmer irrigation records were different, except BIAS. Particularly, the statistical indexes (*r* and

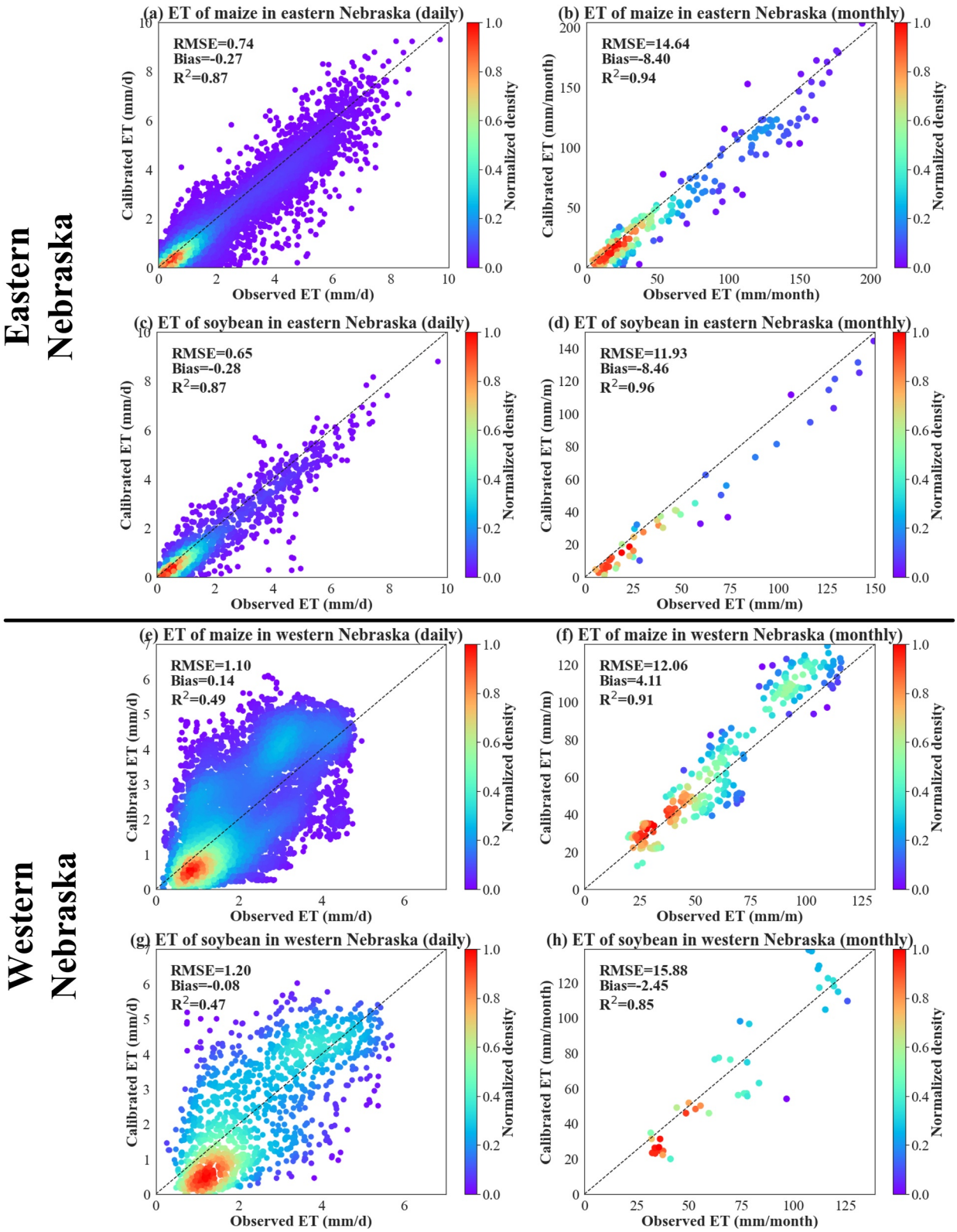

Figure 3. Comparison of observed and calibrated evapotranspiration (ET; daily and monthly) of maize and soybean at the irrigated fields in eastern (a–d) and western (e–h) Nebraska. Black dashed lines indicate the 1-to-1 line. Note that western Nebraska used satellite-based observations and eastern Nebraska used eddy covariance observations.

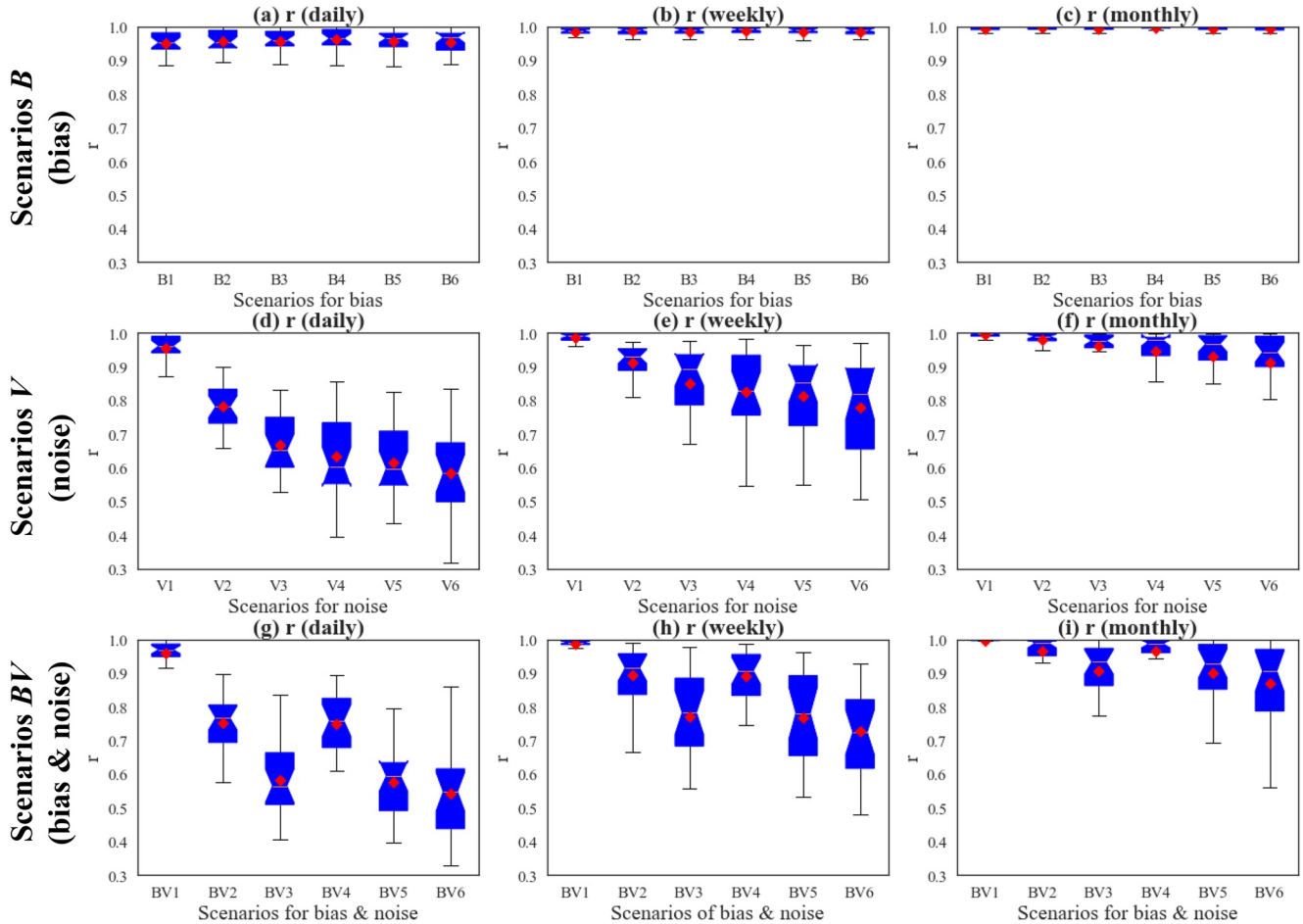

Figure 4. Box plots of Pearson correlation coefficient (r) between estimations of irrigation water use using concurrent configuration and farmer irrigation records at daily, weekly, and monthly scales under scenarios (B, V, BV) at US-Ne1 and US-Ne2 in eastern Nebraska during the period 2001–2012. (a–c) Six scenarios (B_1, B_2, B_3, B_4, B_5, and B_6) investigating the impacts on degrading the estimation performance of irrigation water use resulting from bias. (d–f) Six scenarios (V_1, V_2, V_3, V_4, V_5, and V_6) investigating the impacts on degrading the estimation performance of irrigation water use resulting from noise. (g–i) Six scenarios (BV_1, BV_2, BV_3, BV_4, BV_5, and BV_6) investigating the impacts on degrading the estimation performance of irrigation water use resulting from the combination of bias and noise. Pearson correlation coefficient (r) was calculated for each site-year at different temporal scales (daily, weekly, and monthly).

RMSE) performed the best at the monthly scale but worst at the daily scale, while the statistical index (BIAS) had little difference among different temporal scales (daily, weekly, and monthly).

Taking US-Ne1 (a continuous maize cropping system) in 2004 as an example, CON and SEQ could effectively detect synthetic irrigation records with high accuracy for scenario BV_1 with the combinations of small bias and small noise (1%, 1%) (Figure 6 and Figure S7 in Supporting Information S1). The overlapped irrigation in red bar denoted that the estimations of irrigation water use from CON and SEQ (i.e., irrigation estimations, black bar with hatches) hit farmer irrigation records (blue bar). Daily ET difference between ET simulations from the *ecosys* model before data assimilation (without irrigation impact, red dashed lines) and ET observations (with irrigation impact, blue solid lines) were calculated on each day in real-time. The daily ET differences were removed by incorporating daily irrigation events, thus daily ET simulations from the *ecosys* model before data assimilation without irrigation impact on the target day could be corrected as ET simulations after data assimilation (black solid lines) in real-time with irrigation impact for the next day. Estimations of irrigation water use from CON only missed the irrigation event on 22 July 2004 for 1 day (Figure 6), while SEQ missed irrigation events for 6 days (Figure S7 in Supporting Information S1). It indicated that CON performed slightly better than SEQ for scenario BV_1. Meanwhile, cumulative estimations of irrigation water use was close to cumulative synthetic irrigation records, demonstrating the satisfactory performance of CON and SEQ on estimating irrigation water use at high spatio-temporal resolution (daily and field-scale).

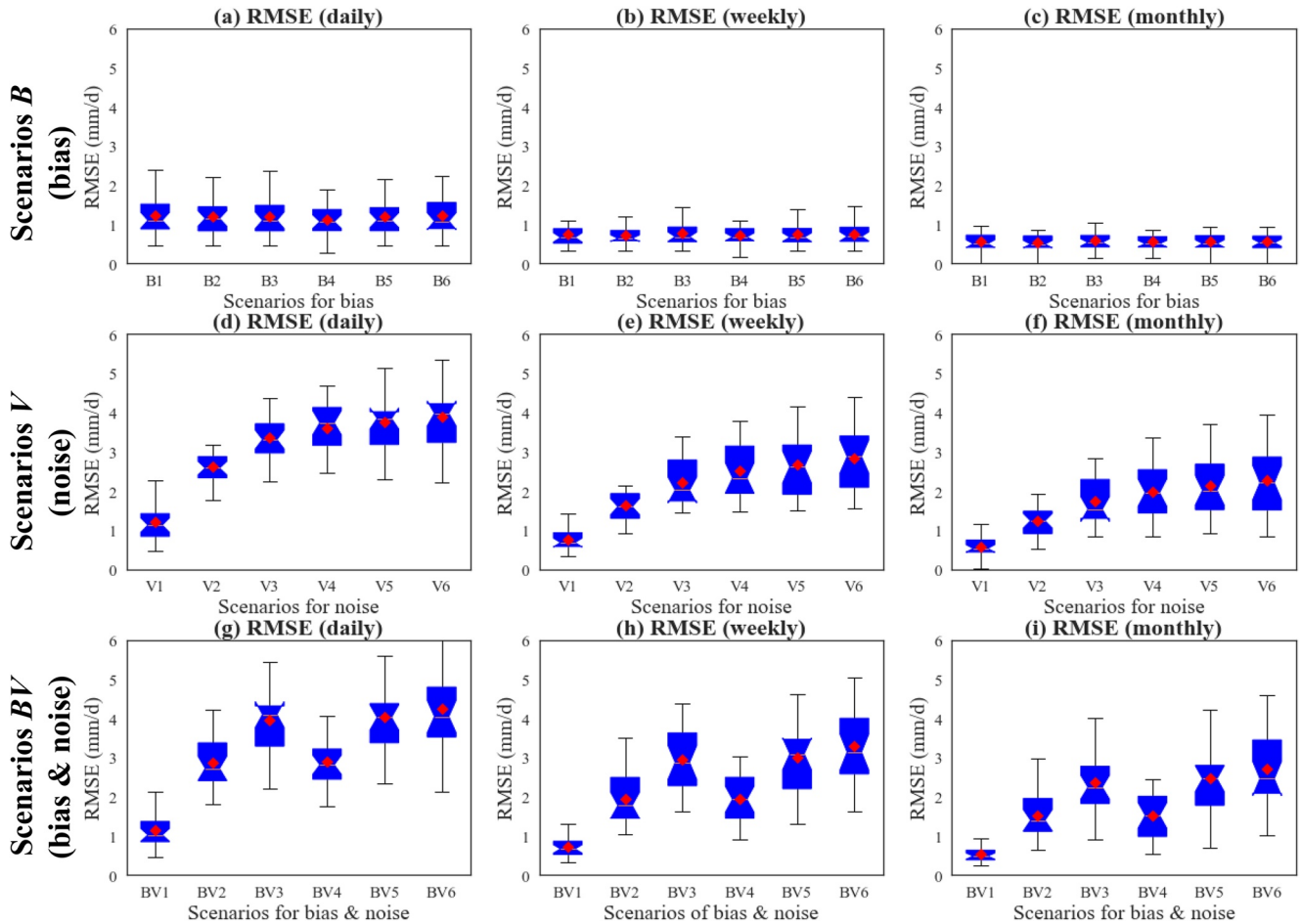

Figure 5. Box plots of RMSE between estimations of irrigation water use using concurrent configuration and farmer irrigation records at daily, weekly, and monthly scales under scenarios (*B*, *V*, *BV*) at US-Ne1 and US-Ne2 in eastern Nebraska during the period 2001–2012. (a–c) Six scenarios (B_1, B_2, B_3, B_4, B_5, and B_6) investigating the impacts on degrading the estimation performance of irrigation water use resulting from bias. (d–f) Six scenarios (V_1, V_2, V_3, V_4, V_5, and V_6) investigating the impacts on degrading the estimation performance of irrigation water use resulting from noise. (g–i) Six scenarios (BV_1, BV_2, BV_3, BV_4, BV_5, and BV_6) investigating the impacts on degrading the estimation performance of irrigation water use resulting from the combination of bias and noise. RMSE were calculated for each site-year at different temporal scales (daily, weekly, and monthly).

4.3. Estimations of Irrigation Water Use Using Real ET Observations in Nebraska

Estimations of irrigation water use using real ET observations was conducted at two sets of irrigated fields in eastern and western Nebraska. Based on the results of the *ecosys* model calibration (Section 4.1), the best distributions of daily ET difference between *ecosys* simulations and observations both with irrigation impact for maize and soybean in eastern and western Nebraska were screened out as Gaussian distributions (Figure S8 in Supporting Information S1). The mean and standard deviation of Gaussian distributions were estimated for bias correction (Equation 4) embedded in particle filtering for estimating irrigation water use. Particle size in the real experiments ($N = 10$) was selected as the same as the synthetic experiments. In addition, three parameters of the proposed model-data fusion framework with CON and SEQ configurations were manually calibrated separately in eastern and western Nebraska, that is, $\alpha = 0.05$, $\beta = 1.5$, $d\mathrm{T} = 3$ in eastern Nebraska and $\alpha = 0.05$, $\beta = 3.0$, $d\mathrm{T} = 7$ in western Nebraska. Irrigation range (β) and irrigation duration ($d\mathrm{T}$) in western Nebraska were larger than those in eastern Nebraska, and this could be explained by climatic differences. Specifically, the climate in western Nebraska (annual precipitation around 450 mm) was much drier than that in eastern Nebraska (annual precipitation around 750 mm), thus requiring more irrigation water use. Based on the calibrated parameters, estimating irrigation water use at high spatio-temporal resolution was conducted by the proposed model-data fusion with CON and SEQ configurations for each site-year in eastern and western Nebraska.

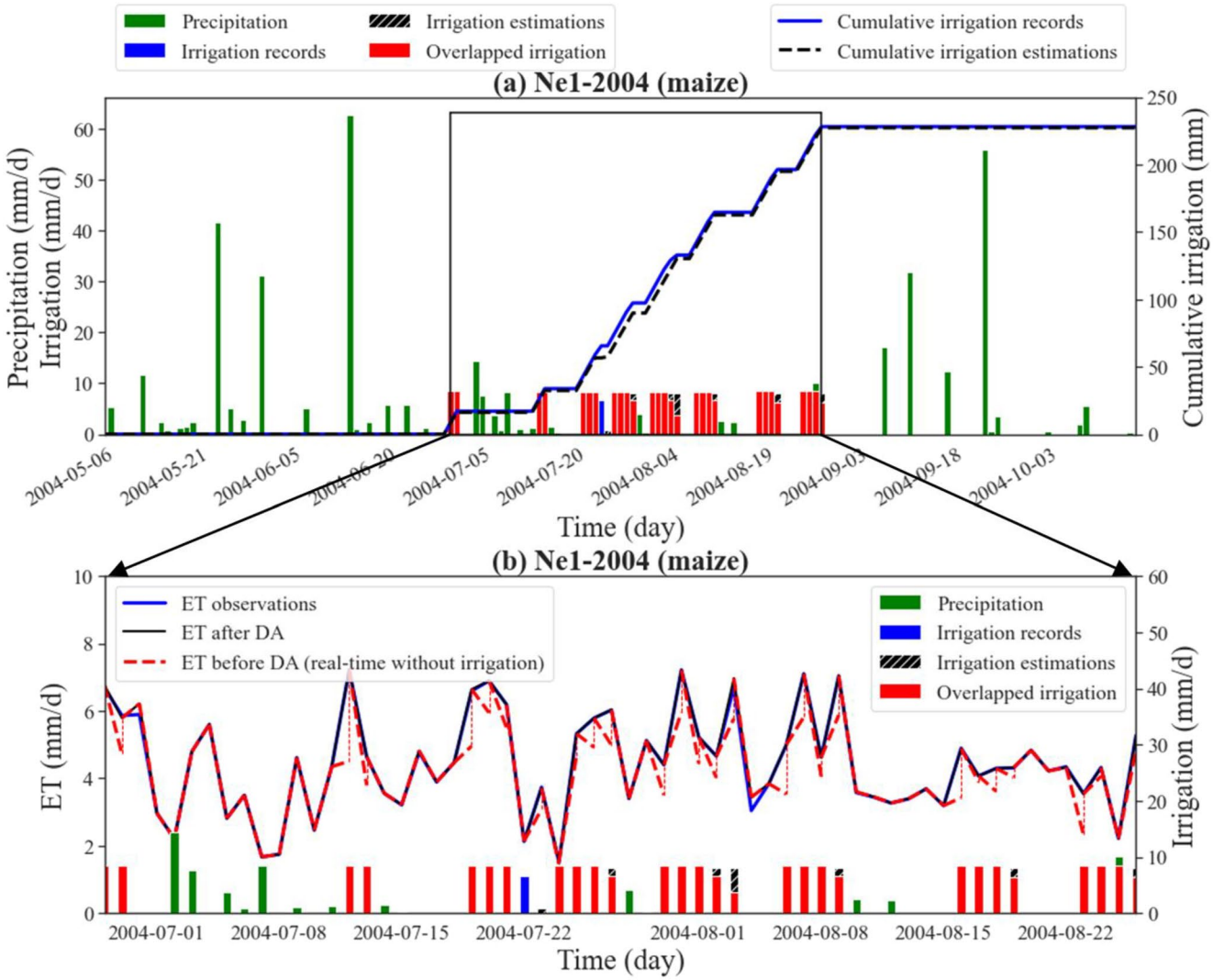

Figure 6. (a) Time series of estimations of irrigation water use using the proposed model-data fusion with concurrent configuration for synthetic experiment of scenario BV_1 (the combinations of low bias, 1%, and low noise, 1%) during the growing season in 2004 at US-Ne1 (a continuous maize cropping system). (b) Time series of evapotranspiration (ET) observations, ET simulations from the *ecosys* model after data assimilation, and ET simulations from the *ecosys* model before data assimilation in real-time without irrigation impact during the irrigation season in 2004 at US-Ne1. The overlapped irrigation (red bar) denoted that the estimations of irrigation water use (i.e., irrigation estimations, black bar with hatches) hit farmer irrigation records (blue bar). ET simulations from the *ecosys* model before data assimilation without irrigation impact on the target day were corrected in real-time with irrigation impact for the next day.

The estimations of irrigation water use at the monthly and annual scales matched well with farmer irrigation records for all the site-years in Nebraska (Figure 7). At the monthly scale, Pearson correlation coefficients of CON and SEQ configurations were 0.80 (p-value < 0.001) and 0.81 (p-value < 0.001), respectively, with bias of 0.19 and −0.88 mm/m (Figure 7a). Both bimodal distributions with the peak around 0 and 100 mm/m were found for farmer irrigation records and estimations of irrigation water use. At the annual scale, 95% confidence intervals of estimations of irrigation water use were very close to the 1-to-1 line, with Pearson correlation coefficients of 0.55 (p-value < 0.001) and 0.47 (p-value < 0.001) for CON and SEQ configurations, respectively (Figure 7b). For the performance comparison between CON and SEQ, we found that SEQ performed better than CON in eastern Nebraska, while there was little difference between CON and SEQ in western Nebraska (Figure 8 and Table 2). For the spatial performance comparison between eastern and western Nebraska, we found that CON and SEQ performed better in eastern Nebraska than those in western Nebraska, that is, higher r and lower RMSE and BIAS in eastern Nebraska (Figure 8 and Table 2). In addition, there was little difference in estimating irrigation water use between fields planted with maize and soybean (Table 2 and Figure S9 in Supporting Information S1).

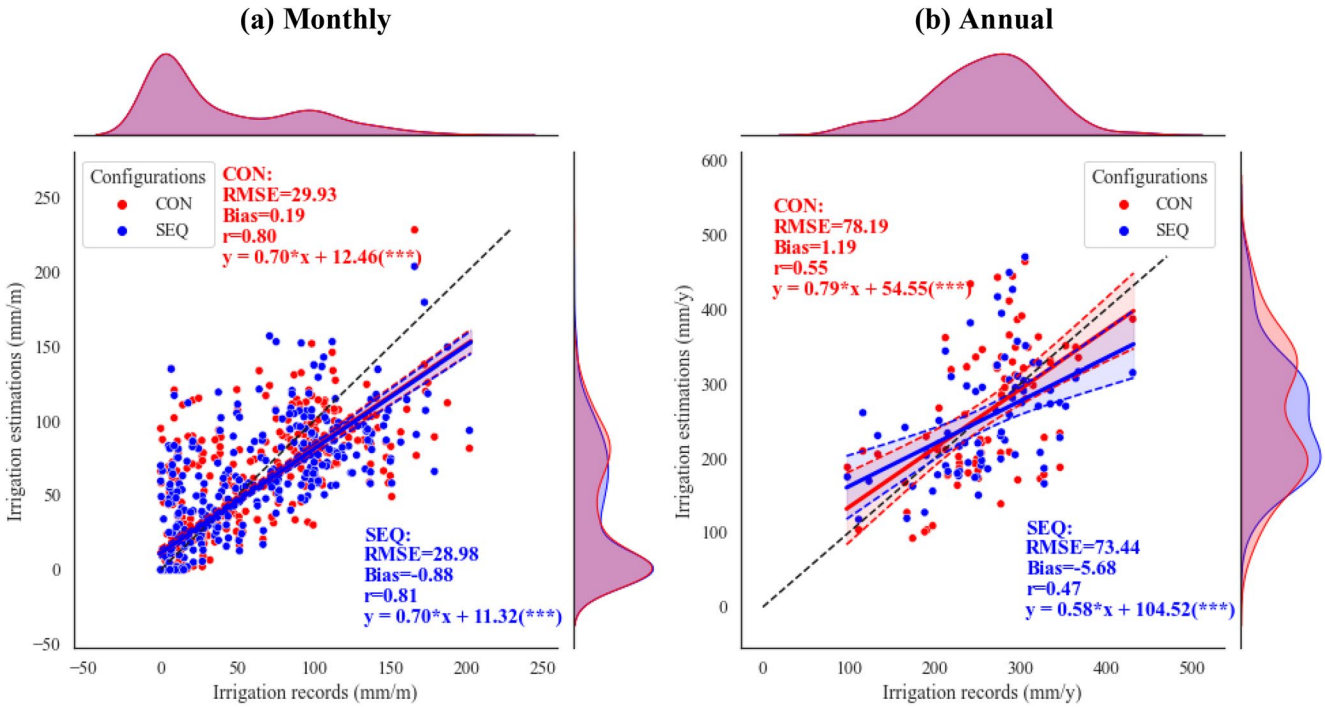

Figure 7. Scatter plots of farmer irrigation records and estimations of irrigation water use at the (a) monthly and (b) annual scales using the proposed model-data fusion framework with concurrent (CON) and sequential (SEQ) configurations across 76 site-years in Nebraska. Black dashed lines indicated the 1-to-1 relationship. Red and blue lines were the regression lines of estimations of irrigation water use with 95% confidence intervals. The *p*-values were represented the symbols (ns meaning $p > 0.05$; * meaning $p \leq 0.05$; ** meaning $p \leq 0.01$; *** meaning $p \leq 0.001$). The probability density functions in the top and right sides denoted the kernel density estimations of farmer irrigation records and estimations of irrigation water use.

Taking the fields (1013503, 1011702, and 1011960) which grew maize in 2015 in western Nebraska as examples, the model-data fusion with CON and SEQ configurations successfully detected most of the irrigation events at the daily scale (the overlapped irrigation events, red bar) but still with some missing (blue bar) or redundant irrigation events (black bar with hatches) (Figure 9, and Figures S10–S14 in Supporting Information S1). The daily ET difference between model simulations before data assimilation (without irrigation impact, red dashed lines) and daily ET observations (with irrigation impact, blue solid lines) were used for irrigation detection in real time (Figure 9, and Figures S10–S14 in Supporting Information S1). Then, 10 irrigation particles with different amounts in the particle filtering were incorporated into the *ecosys* model to account for the impacts of irrigation with different amounts in real-time on each day (Figure S15 in Supporting Information S1). The final daily irrigation amount was determined by the weighted average of all the irrigation particles, and it was assimilated into the *ecosys* model to remove the ET difference in real-time. Thus, daily ET simulations from the *ecosys* model before data assimilation without irrigation impacts (red dashed lines) could be updated into ET simulations after data assimilation with irrigation impacts (black solid lines) in real-time. In addition, the 95% confidence interval of cumulative estimations of irrigation water use based on 10 replicates were narrow and covered cumulative farmer irrigation records for most time periods (Figure 9, and Figures S10–S14 in Supporting Information S1). All these results demonstrated that the proposed model-data fusion with CON and SEQ configurations were robust and reliable for estimating irrigation water use at high spatio-temporal resolution.

The total deviation from remotely sensed ET and precipitation during the growing seasons (i.e., the estimation of minimum irrigation water use based on water balance ($I_{\min} = \max[ET_{obs} - P_{obs}, 0]$)) (Irmak et al., 2011; Van Dijk et al., 2018) was compared with the estimations of irrigation water use based on CON and SEQ configurations and actual irrigation records applied by farmers (Figure 10). The boxplots indicated that the estimation of minimum irrigation water use based on water balance (mean: 120.59 and 73.92 mm/yr in eastern and western Nebraska) were much lower than the estimations of irrigation water use using CON (mean: 195.22 and 284.26 mm/yr in eastern and western Nebraska) and SEQ (mean: 243.60 and 258.31 mm/yr in eastern and western Nebraska) and farmer irrigation records (mean: 226.14 and 274.67 mm/yr in eastern and western Nebraska;

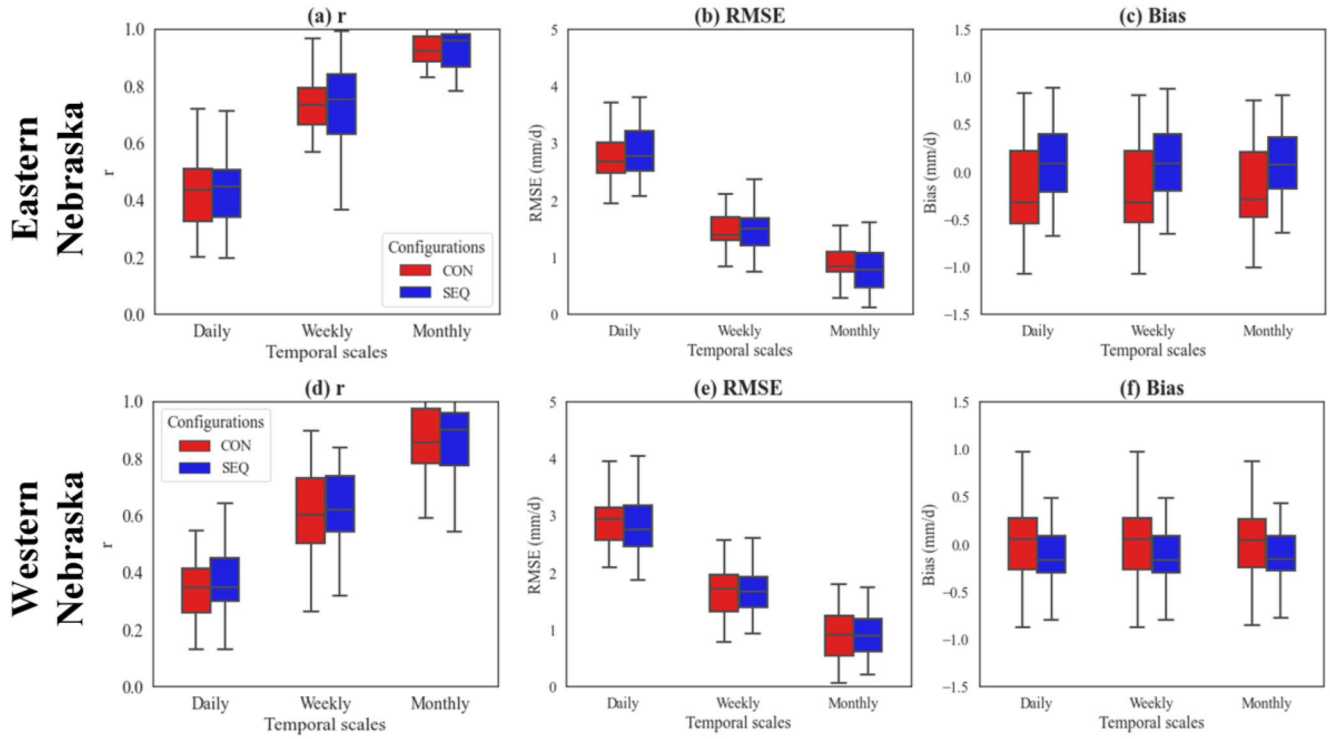

Figure 8. Box plots of the statistical indexes (*r*, RMSE, and BIAS) of estimations of irrigation water use using the proposed model-data fusion framework with concurrent (CON) and sequential (SEQ) configurations at different temporal scales (daily, weekly, and monthly) for all site-years in (a–c) eastern and (d–f) western Nebraska. The statistical indexes were calculated for each site-year. There were 24 and 52 site-years in eastern and western Nebraska, respectively.

Figures 10a and 10c). The estimations of irrigation water use based on CON and SEQ configurations were close to the farmer irrigation records in eastern and western Nebraska. It indicated that our proposed model-data fusion framework with CON and SEQ configurations was reliable for the estimations of irrigation water use. In addition, we analyzed the relationships between irrigation water use and precipitation during the growing seasons to check the sensitivity of irrigation water use to climate variability (Figures 10b and 10d). Irrigation water use decreased with the increasing precipitation, which were reflected in four cases ($r < 0$), indicating that irrigation water use was smaller in wet years with higher precipitation, especially in eastern Nebraska ($r = -0.60$). We also found that the fitted regression lines with 95% confidence intervals of the estimations of irrigation water use based on CON and SEQ were close to those of farmer irrigation records in eastern and western Nebraska, further demonstrating

Table 2
The Statistical Indexes (r, RMSE, and BIAS) of the Estimations of Irrigation Water Use Using the Proposed Model-Data Fusion Framework With Concurrent (CON) and Sequential (SEQ) Configurations at Different Temporal Scales (Weekly, Monthly, and Annually) in the Irrigated Fields Planted With Maize and Soybean in Eastern and Western Nebraska

		Eastern Nebraska			Western Nebraska			Maize			Soybean		
Temporal scales	Methods	*r* (*p*-value)	BIAS (mm)	RMSE (mm)	*r* (*p*-value)	BIAS (mm)	RMSE (mm)	*r* (*p*-value)	BIAS (mm)	RMSE (mm)	*r* (*p*-value)	BIAS (mm)	RMSE (mm)
Weekly	CON	0.68 (***)	−1.26	11.30	0.56 (***)	0.37	12.41	0.60 (***)	−0.34	11.95	0.63 (***)	1.60	12.81
	SEQ	0.70 (***)	0.71	11.40	0.58 (***)	−0.63	12.11	0.62 (***)	−0.36	11.85	0.65 (***)	0.72	12.22
Monthly	CON	0.82 (***)	−5.01	30.83	0.78 (***)	1.47	29.79	0.80 (***)	−1.34	29.66	0.79 (***)	6.29	32.27
	SEQ	0.86 (***)	2.83	27.48	0.78 (***)	−2.50	29.61	0.81 (***)	−1.45	28.86	0.81 (***)	2.84	29.75
Annual	CON	0.45 (*)	−30.92	90.23	0.48 (***)	9.59	75.36	0.50 (***)	−8.64	78.36	0.81 (**)	40.24	87.78
	SEQ	0.61 (**)	17.46	72.02	0.38 (**)	−16.36	74.09	0.43 (***)	−9.29	72.54	0.69 (*)	18.15	79.14

Note. The *p*-values were represented the symbols (ns meaning $p > 0.05$; * meaning $p \leq 0.05$; ** meaning $p \leq 0.01$; *** meaning $p \leq 0.001$). There were 24 and 52 site-years in eastern and western Nebraska, respectively. There were 66 and 10 site-years planted with maize and soybean in Nebraska, respectively.

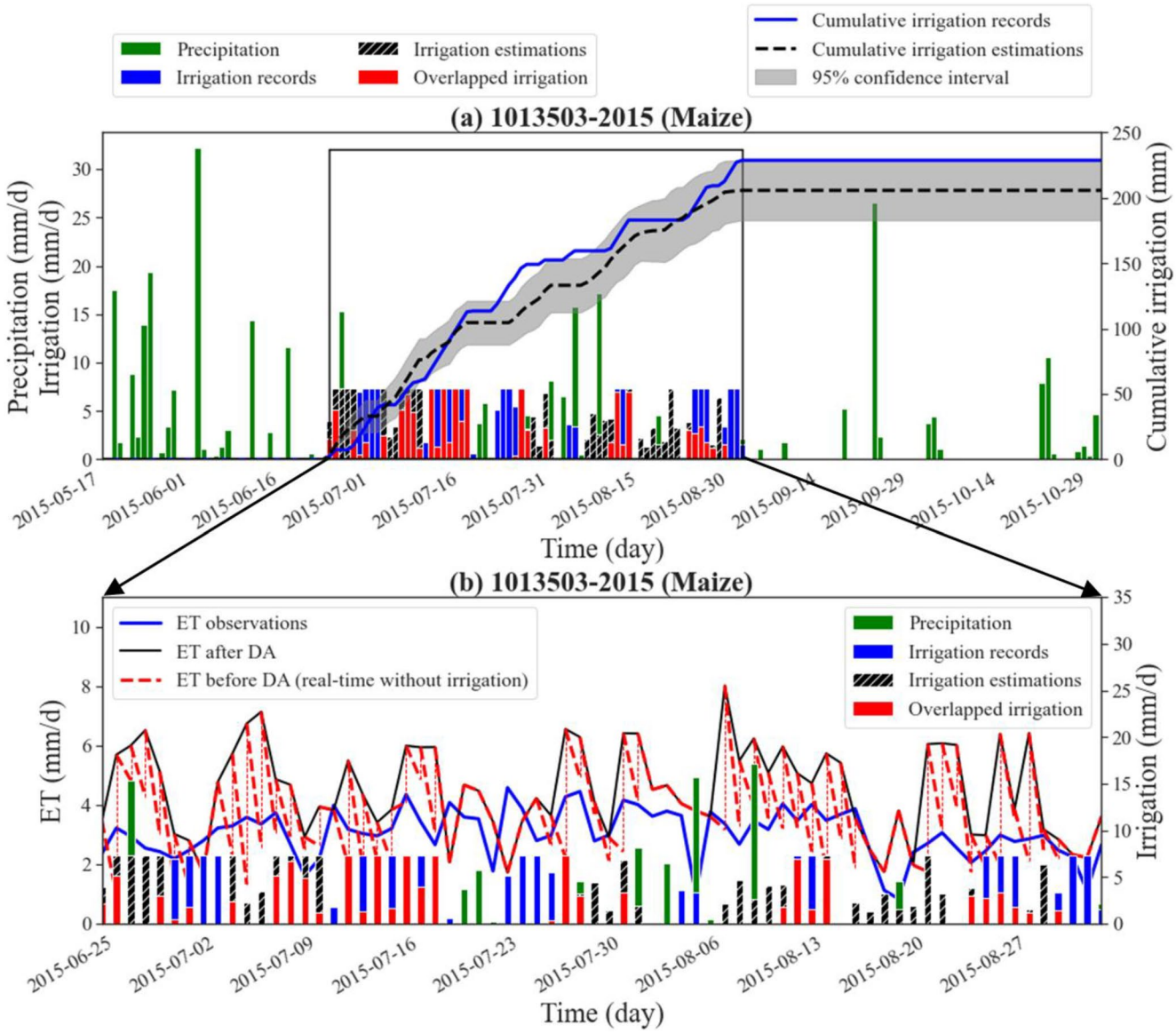

Figure 9. (a) Time series of estimations of irrigation water use using the proposed model-data fusion with sequential configuration at the field (1013503) which grew maize during the growing season in 2015 in western Nebraska. (b) Time series of evapotranspiration (ET) observations, ET simulations from the *ecosys* model after data assimilation, and ET simulations from the *ecosys* model before data assimilation in real-time without irrigation impact at the field (1013503) during the irrigation season in 2015 in western Nebraska. The overlapped irrigation (red bar) denoted that the estimations of irrigation water use (i.e., irrigation estimations, black bar with hatches) hit farmer irrigation records (blue bar). ET simulations from the *ecosys* model before data assimilation without irrigation impact on the target day were corrected in real-time with irrigation impact for the next day. The gray area denoted 95% confidence interval of cumulative estimations of irrigation water use with 10 replicates.

the reliability of the proposed model-data fusion framework with CON and SEQ configurations for estimating irrigation water use.

In addition, the difference between farmer irrigation records and the water balance case could be treated as water loss unavailable for crop use (water loss = max[I_{obs} + P_{obs} − ET_{obs}, 0]) from five potential sources, including runoff, deep percolation, air evaporation, plant interception, and leakage in the irrigation systems, ignoring the change of soil water storage (Irmak et al., 2011; Van Dijk et al., 2018). For the water balance case, we found that about one-third (33.56%) of available water (including precipitation and irrigation) was not used by crops across all the site-years (2015–2016 at 29 fields) located in Keith and Deuel counties in western Nebraska. The unused water fraction (33.56%) in western Nebraska was larger than that during 2001–2012 at two AmeriFlux sites

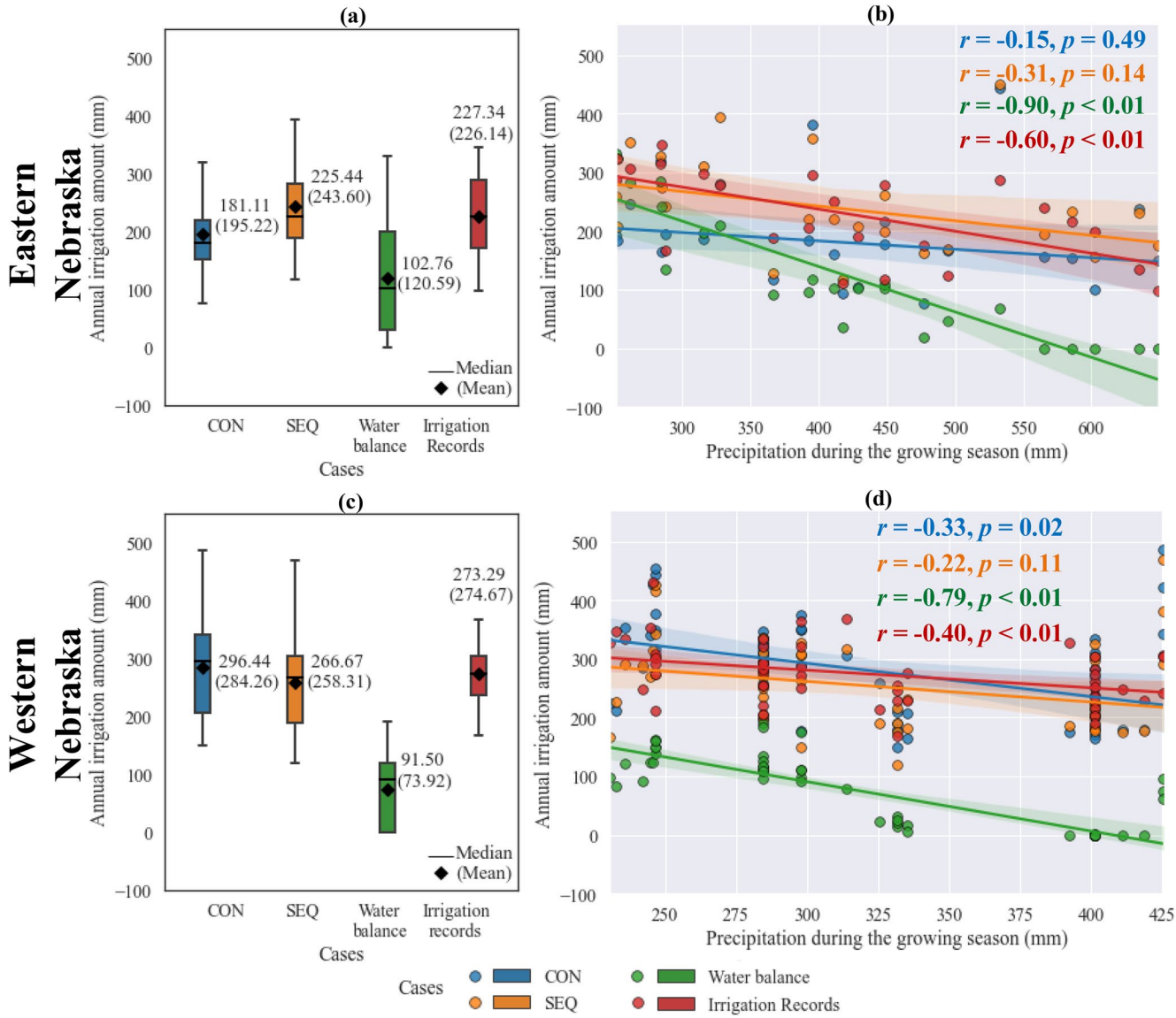

Figure 10. The comparison of field-scale irrigation water use among four cases (concurrent [CON], sequential [SEQ], water balance, irrigation records) during the growing seasons at all site-years in eastern and western Nebraska. Boxplots of irrigation water use from four cases at all site-years in (a) eastern and (c) western Nebraska. Relationships between irrigation water use from four cases and precipitation during the growing seasons in (b) eastern and (d) western Nebraska. CON and SEQ denoted the estimations of irrigation water use using the proposed model-data fusion framework with CON and SEQ configurations, respectively. Water balance denoted the estimations of irrigation water use based on water balance, that is, $I_{\min} = \max[ET_{obs} - P_{obs}, 0]$. Irrigation records represented the recorded irrigation water use applied by farmers for each site-year. The lines in (b and d) denoted the regression lines with 95% confidence intervals. r and p were Pearson correlation coefficients and p-values, respectively.

(US-Ne1 and US-Ne2) (17.47%) in eastern Nebraska. It was consistent with previous studies that total irrigation water use in Nebraska could potentially be reduced up to 25%–40% without hurting crop yields (K. E. Gibson et al., 2019). In addition, we found that water loss increased with precipitation (Figures 10b and 10d), indicating that farmers applied more excess irrigation with higher precipitation during the growing seasons. All these results suggested that the farmers' irrigation behavior at the research fields in Nebraska might be suboptimal for water saving, especially at the irrigated fields in western Nebraska. Thus, there should be a large opportunity to improve irrigation efficiency in Nebraska by adopting more efficient irrigation scheduling technologies (J. Zhang et al., 2021b; J. Zhang et al., 2021c).

5. Discussion

5.1. Impacts of ET Uncertainties on the Efficacy of the Proposed Model-Data Fusion

The proposed model-data fusion approach with CON and SEQ configurations for estimating center-pivot irrigation water use at high spatio-temporal resolution (daily and field-scale) is successfully applied in synthetic and real experiments at two sets of irrigated fields in eastern and western Nebraska. The fundamental theory behind this approach to estimate center-pivot irrigation water use is the difference between remotely sensed ET observations with irrigation impacts and ET simulations from the process-based *ecosys* model without irrigation impacts. The daily irrigation events are estimated by assimilating the remotely sensed ET observations into the *ecosys* model via particle filtering with multiple irrigation events. Thus, the uncertainties of observed and simulated ET have critical impacts on the efficacy of the proposed model-data fusion approach with CON and SEQ configurations.

If there are relatively small uncertainties in the remotely sensed ET observations and ET simulations from the *ecosys* model, the ET difference can largely be attributed to the irrigation, and our proposed model-data fusion can effectively detect all the irrigation events, as shown in the synthetic experiment of scenario BV_1 (the combinations of low bias, 1%, and low noise, 1%) in Figure 6. However, the uncertainties in the ET observations and simulations are unavoidable and unquantifiable. In this study, we combine the uncertainties from process-based model and observations together, and attribute the ET uncertainties into two sources (i.e., bias and noise). The ET uncertainties are represented by the Gaussian distribution (bias, μ_{s-o}, and standard deviation, i.e., noise, σ_{s-o}) of ET difference between the simulations from the calibrated process-based model and remotely sensed observations both with irrigation impact. The synthetic experiments (i.e., three groups of scenarios including bias-*B*, noise-*V*, and bias and noise-*BV*) indicated that the ET uncertainties with noise had larger impacts on degrading the performance of the proposed model-data fusion to estimate irrigation water use than those with bias. The reason is that bias correction embedded in particle filtering could effectively remove the ET uncertainties resulting from bias, while the ET uncertainties resulting from noise is difficult to be removed via particle filtering.

For the ET uncertainties in the real experiments, the noise (i.e., standard deviation) in eastern Nebraska is smaller than that in western Nebraska for maize and soybean (Figure S8 in Supporting Information S1). Thus, the proposed model-data fusion approach with CON and SEQ configurations has better performance on the estimations of irrigation water use in eastern Nebraska with smaller ET uncertainties than that in western Nebraska with larger ET uncertainties. The fundamental reason for smaller ET uncertainties in eastern Nebraska (i.e., smaller noise in eastern Nebraska in Figure S8 in Supporting Information S1) is that the irrigated fields (US-Ne1 and US-Ne2) in eastern Nebraska use the eddy covariance-based ET observations and ET simulations from the *ecosys* model with the complete field management data sets from UNL-ENREC's CSP, while the irrigated fields in western Nebraska use the satellite-based BESS-STAIR ET observations and ET simulations from the *ecosys* model without detailed field management data sets. Note that the irrigated fields in western Nebraska are more realistic compared to the irrigated fields (US-Ne1 and US-Ne2) in eastern Nebraska, which have the gold standard of scientific observations. For most irrigated fields, the BESS-STAIR ET data set can be used as ET observations, while the management information is usually unknown due to lack of open access, technological knowledge, or held by private companies, which increases the ET uncertainties for the estimations of irrigation water use.

5.2. Uncertainty Reduction Pathways

This study has demonstrated that the ET uncertainties have significant negative impacts on the efficacy of the proposed model-data fusion with CON and SEQ configurations for the estimations of irrigation water use. We will discuss the possible pathways for reducing the uncertainties from both data and model perspectives. From the data perspective, ET observations with higher accuracy could reduce the ET uncertainties and improve the estimations of irrigation water use. For example, the real experiments for estimating irrigation water use using eddy covariance measurements of ET in eastern Nebraska performed better than those using satellite-based BESS-STAIR ET measurements in western Nebraska (Figure 8 and Table 2). The reason was that ET observations from eddy covariance measurements were more accurate than the satellite-based ET observations. It further confirmed the importance of ET observations for estimating irrigation water use based on the model-data fusion framework. To improve remotely sensed ET observations can be possibly achieved by constraining the satellite-based ET models (Courault et al., 2005) with LST data set, as LST reflects the cooling effects due to

irrigation and in turn can be used to improve ET observations (J. Zhang et al., 2021a). However, the existing satellite-based LST data sets usually could not fulfill high resolutions in space and time simultaneously; for example, MODIS LST data is at the daily step (snapshot) but at 1 km resolution; Landsat LST resampled data is at 30 m resolution but has 16-day interval; and ECOSTRESS LST data is at 70 m resolution but has irregular revisit time (Cook, 2014; Cook et al., 2014; Li et al., 2021). In addition, existing global satellite LST products generally show large daytime uncertainties (e.g., bias = 2°C and RMSE = 3.5°C) in croplands (Li et al., 2021), which might be propagated to ET observations. More advanced satellite thermal sensors (Wright et al., 2020), multi-satellite LST fusion algorithms (Xu & Cheng, 2021), and data-model fusion algorithms (X. Zhang, Zhou, et al., 2021) will potentially lead to the development of high-quality LST products at high spatio-temporal resolution in the future, ultimately for remotely sensed ET data sets with high accuracy.

The possible pathways from the model perspective (including inputs, process, and parameters) for reducing the uncertainties will be discussed here. (a) More detailed field-scale management data collection (such as planting date, fertilizer records, and irrigation systems) could effectively reduce the uncertainties of model simulations of ET and thus improve the estimations of irrigation water use (Massari et al., 2021). Especially, irrigation seasons (starting and ending day) could effectively improve the estimations of irrigation water use. Irrigation seasons are determined based on farmer irrigation records in this study, while they are usually unknown at large-scale and need more investigation in the future. The year-specific irrigation seasons could be approximated based on local farmers' experience and year-specific climate rainfall information, such as mid-June to mid-September for maize in 2022 at North Platte, western Nebraska (UNL, 2022). (b) Advanced ecosystem models with full physical mechanisms, such as plant hydraulics and plant growth fulfilled in the *ecosys* model, could improve crop water use (i.e., ET) simulations, thus accurate ET difference between observations and simulations could help for estimating irrigation water use. (c) Parameters related to crop phenology, photosynthetic, and soil hydrological properties in the ecosystem models had large impacts on ET simulations. More reliable and high-fidelity observations, such as remotely sensed GPP and LAI data sets (C. Jiang et al., 2021; Kimm et al., 2020; Wu et al., 2020), could be applied to constrain these parameters in the ecosystem models to obtain reliable crop water use and hydrological simulations.

5.3. Implications of the Current Study

Estimating irrigation water use at high spatio-temporal resolution in this study can contribute to sustainable regional water management and understanding groundwater depletion for sustainable groundwater management in groundwater-dependent irrigated regions. The proposed model-data fusion framework for estimating irrigation water use can be applied in the irrigated agricultural lands with different crops and/or multiple cropping systems at large-scale. The remotely sensed BESS-STAIR ET, GPP, and LAI data sets at high-spatiotemporal resolutions (daily and field-scale) can be used to constrain the process-based models at large-scale. However, the parameters (ET difference threshold and irrigation duration) need to be calibrated with some necessary information, such as the field-scale irrigation water use at some sample fields or total irrigation water use at large-scale regions. The application of this model-data fusion framework to estimate irrigation water use can be treated as water footprint estimation in the irrigated lands. Current existing water footprint data sets have coarse spatial and temporal resolutions, and our study can provide water footprint data sets at the daily and field scale. Long-term water footprint data sets can be used to investigate the spatio-temporal variability of irrigation efficiency, thus to evaluate different irrigation conservation programs, such as the Local Enhanced Management Area program in Kansas (Deines et al., 2021) and the widespread adoption of low-energy precision application technologies (McCarthy et al., 2020). Then, potential regions with low irrigation efficiency but water scarcity can be identified to reform regional water policies to regulate farmers' irrigation water use for sustainable water management (Foster et al., 2020; D. Wang & Cai, 2007). In addition, water footprint data sets at high spatio-temporal resolution can be used to understand groundwater pumping and recharge rate patterns for long-term aquifer conservation in groundwater-dependent irrigated regions, such as the High Plains Aquifer (HPA). Agriculture in Nebraska, Kansas, and Texas largely depends on groundwater pumping in the HPA for irrigation, but there is large spatial variability for the groundwater level changes, that is, slight groundwater level declines in northern HPA (Nebraska) while serious groundwater level declines in southern HPA (Kansas and Texas; Nie et al., 2018; Scanlon et al., 2012). Application of our methods in HPA may provide a pathway to investigate the primary causes of the disparities for groundwater level changes and the possible strategies for groundwater sustainability in the HPA.

Estimating irrigation water use at high spatio-temporal resolution can also help farmers to achieve sustainable irrigation. The proposed method in this study can effectively reflect farmers' irrigation behavior, thus its applications at large-scale can be used to understand the spatio-temporal variability of farmers' irrigation practices and to estimate water loss fractions unavailable for crop use (Foster et al., 2019). Water loss fractions (such as around one-third in western Nebraska) can indicate how much space is left for irrigation improvements. Thus, estimating irrigation water use at high spatio-temporal resolution can help to improve farmers' irrigation practices with more science-based irrigation methods in regions with low irrigation efficiencies and high water loss fractions (J. Zhang et al., 2021b; J. Zhang et al., 2021c). In addition, estimations of irrigation water use can compensate for the missing irrigation records if farmers do not provide, then accurate soil water budgets at the field level can be provided for precision irrigation with the estimations of irrigation water use as past water inputs. Furthermore, accurate soil water budgets with the estimations of irrigation water use can also help to estimate ecosystem carbon, energy, and nitrogen budgets, thus for modeling crop growth and precision nitrogen management.

Last but not least, the estimations of irrigation water use (irrigation timing and amount) in this study can help the ecosystem and hydrological models to track terrestrial water and energy cycles in the irrigated regions. Irrigation is the major anthropogenic disturbance of terrestrial water and energy cycles in the irrigated agricultural lands (McDermid et al., 2021), as irrigation performs as water inputs and affects surface energy budget (i.e., energy partitioning between latent and sensible heat fluxes). The estimations of irrigation water use reflecting farmers' irrigation behavior in this study can be used to investigate the direct impacts of irrigation on regional water and energy budgets with land-atmosphere feedbacks. The traditional criterion-based irrigation scheduling (such as maximum allowable depletion, MAD-50%) set in the ecosystem and hydrological models cannot reflect farmers' irrigation decisions (de Rosnay et al., 2003; Haddeland et al., 2006), as farmers' irrigation decisions are complicated due to many factors, such as irrigation infrastructures, farmers' preferences, and climate conditions (Foster et al., 2020; D. Wang & Cai, 2007). The proposed method in this study offers a pathway to estimate irrigation water use at high spatio-temporal resolution reflecting farmers' irrigation behavior.

6. Conclusions

We have demonstrated that our proposed model-data fusion framework with CON and SEQ configurations is effective for estimating center-pivot irrigation water use at the daily and field scale. The irrigation signals are detected by the difference between remotely sensed ET observations with irrigation impacts and ET simulations from the agroecosystem (*ecosys*) model without irrigation impacts. The uncertainties of remotely sensed ET observations and ET simulations from the *ecosys* model have critical impacts on the efficacy of the proposed model-data fusion approach with CON and SEQ configurations. We conclude two major findings based on two types of experiments using synthetic and real ET observations in Nebraska: (a) Three groups of scenarios (bias-*B*, noise-*V*, and bias and noise-*BV*) for the synthetic experiments indicated that, among two sources of ET uncertainties (bias and noise), noise had larger impacts on degrading the performance of the proposed model-data fusion to estimate irrigation water use than those with bias. Systematic bias can be removed by bias correction embedded in the particle filtering. (b) The proposed model-data fusion framework with CON and SEQ configurations offered a pathway to estimate center-pivot irrigation water use at high spatio-temporal resolution. The estimations of irrigation water use at the monthly and annual scales matched well with farmer irrigation records, with RMSE less than 30 mm/m and 80 mm/yr, absolute BIAS less than 1 mm/m and 6 mm/yr, and r around 0.80 and 0.50, respectively. Although detecting daily irrigation records was very challenging, our method still gave a good performance with RMSE, BIAS, and r around 2.90, 0.03, and 0.4 mm/d, respectively. The proposed model-data fusion framework for estimating irrigation water use at high spatio-temporal resolution could contribute to regional water management, sustainable irrigation, and better tracking terrestrial water and energy cycles.

Appendix A

Ecosys, an advanced agroecosystem model based on biophysical and biochemical mechanisms, uses the multi-layered soil-root-canopy system to track the water, energy, carbon, and nutrient cycles (Grant, 1995, 1997; Grant et al., 1993). *Ecosys* can simulate major agricultural management practices, including irrigation (Grant et al., 2007, 2004), fertilizer (Grant, Juma, Robertson, Izaurralde, & McGill, 2001), crop rotation (Grant, 1997), and tillage (Grant, 1997), which has been extensively validated in many agricultural ecosystems (Grant, 1995; Grant et al., 2007; Grant & Flanagan, 2007; Grant et al., 2001, 2011, 1993, 1999; Mezbahuddin et al., 2020;

Zhou et al., 2021). The hourly crop water uptake, carbon assimilation, and energy fluxes are determined through the hourly two-stage convergence of canopy temperature and canopy water potential in the first and second stages, respectively. Canopy temperature (T_c) is calculated for the first-order closure of canopy energy balance (Equation A1), including canopy net radiation ($R_{n(c)}$), canopy latent heat (LE_c, Equation A2), canopy sensible heat (H_c, Equation A4), and canopy heat storage (G_c, Equation A5). There are two sources for the canopy LE_c, including canopy evaporation from free water on crop leaf surfaces (LE_{c-e}, Equation A3a) and canopy transpiration (LE_{c-t}, Equation A3b). Then, canopy water potential (ψ_c) is calculated for canopy water balance between root water uptake from multiple soil layers and capacitance (left term in Equation A6) and canopy transpiration (right term in Equation A6) based on the closure of canopy energy balance. Canopy transpiration is jointly controlled by aerodynamic resistance (r_a) and canopy stomatal resistance (r_c), which is controlled by two mechanisms, including canopy photosynthesis and canopy turgor potential. In addition to the net radiation retained by the canopy ($R_{n(c)}$), the remaining net radiation is retained by soil surface ($R_{n(g)}$), and fulfilled the closure of soil energy balance (Equation A7). The soil surface latent heat (LE_g) includes two sources (Equation A8): the evaporation from surface litter (LE_{g-l}, Equation A9a) and the evaporation from soil surface (LE_{g-s}, Equation A9b). More details about the soil-plant water relations in *ecosys* can be found in Grant et al. (2020, 1999).

Canopy energy exchange:

$$R_{n(c)} + LE_c + H_c + G_c = 0 \tag{A1}$$

$$LE_c = LE_{c-e} + LE_{c-t} \tag{A2}$$

$$LE_{c-e} = F_c L\upsilon(e_a - e_c)/r_a \tag{A3a}$$

$$LE_{c-t} = F_c L\upsilon(e_a - e_c)/(r_a + r_c) \tag{A3b}$$

$$H_c = F_c C_a(T_a - T_c)/r_a \tag{A4}$$

$$G_c = C_c(T_{c(t-1)} - T_{c(t)}) \tag{A5}$$

$$\sum_n(\psi_c - \psi_{s,n}) / (r_{s,n} + r_{r,n} + r_{a,n}) + X_c\delta\psi_c/\delta t = (e_a - e_c)/(r_a + r_c) \tag{A6}$$

Soil surface energy exchange:

$$R_{n(g)} + LE_g + H_g + G_g = 0 \tag{A7}$$

$$LE_g = LE_{g-l} + LE_{g-s} \tag{A8}$$

$$LE_{g-l} = L(e_a - e_{g-l})/r_{g-l} \tag{A9a}$$

$$LE_{g-s} = L(e_a - e_{g-s})/r_{g-s} \tag{A9b}$$

where F_c is the fraction of shortwave irradiance retained by the canopy (m^2 canopy area m^{-2} ground area); L is the latent heat of water evaporation (MJ m^{-3}); υ is the specific volume of water (m^3 Mg^{-1}); e_a is atmospheric vapor density at air temperature and ambient humidity; e_c is canopy vapor density at T_c and ψ_c; C_a is heat capacity of atmosphere (MJ m^{-3} K^{-1}); T_a is air temperature (K); C_c is areal heat capacity of the canopy (MJ m^{-2} K^{-1}); ψ_s is the water potential in soil layer n; $r_{s,n}$ is the radial resistance from soil to root surfaces in soil layer n; $r_{r,n}$ is the radial resistance from those surfaces to root axes in soil layer n; $r_{a,n}$ is the axial resistances from root axes to canopy in soil layer n; X_c is canopy capacitance; H_g and G_g represent the soil sensible heat and soil heat storage, respectively; e_{g-l} and e_{g-s} represent the surface litter vapor density and the soil surface vapor density, respectively; and r_{g-l} and r_{g-s} represent the surface litter boundary layer resistance and the soil surface boundary layer resistance, respectively.

Conflict of Interest

The authors declare no conflicts of interest relevant to this study.

Data Availability Statement

Ecosys can be freely downloaded from GitHub (https://github.com/jinyun1tang/ECOSYS; Tang & Grant, 2020). The field measurements (including irrigation records) at two irrigated fields (US-Ne1 and US-Ne2) in eastern Nebraska can be freely accessed from http://fluxnet.fluxdata.org/data/fluxnet2015-dataset/ (Pastorello et al., 2020). Actual farmer irrigation records at 29 irrigated fields in western Nebraska are collected from AgSense and FieldNET irrigation software provided by the Nebraska Chapter of The Nature Conservancy through the Western Nebraska Irrigation Project. The meteorological variables from the North American Land Data Assimilation System (NLDAS-2) can be freely accessed from https://ldas.gsfc.nasa.gov/nldas/v2/forcing (NASA, 2022). The soil information from the Gridded Soil Survey Geographic Database (gSSURGO) data sets can be freely accessed from https://data.nal.usda.gov/dataset/gridded-soil-survey-geographic-database-gssurgo (Staff, 2022). The BESS-STAIR ET data sets (daily and field-scale) during the growing seasons from 2015 to 2016 at 29 fields in western Nebraska used in the real experiments are shared via GitHub (https://github.com/Jingwenzhang92/BESS-STAIR-ET), and are deposited in Zenodo permanently (https://doi.org/10.5281/zenodo.7251009; C. Jiang & Zhang, 2022).

Acknowledgments
The authors acknowledge the support from USDA National Institute of Food and Agriculture Foundational Program Cyber-physical systems (2019-67021-29312) and NSF CAREER award (1847334) managed through the NSF Environmental Sustainability Program. Access to field sites and data sets in Western Nebraska was provided by The Nature Conservancy, the Western Nebraska Irrigation Project, and the South Platte Natural Resources District. Funding for the AmeriFlux core sites was provided by the U.S. Department of Energy's Office of Science. This research was a contribution from the Long-Term Agroecosystem Research (LTAR) network. LTAR is supported by the United States Department of Agriculture. T.E.F. acknowledges the financial support of the USDA National Institute of Food and Agriculture, Hatch project (1020768).

References

Abolafia-Rosenzweig, R., Livneh, B., Small, E. E., & Kumar, S. V. (2019). Soil moisture data assimilation to estimate irrigation water use. *Journal of Advances in Modeling Earth Systems*, *11*(11), 3670–3690. https://doi.org/10.1029/2019ms001797

Abrahart, R. J., & See, L. (2002). Multi-model data fusion for river flow forecasting: An evaluation of six alternative methods based on two contrasting catchments. *Hydrology and Earth System Sciences*, *6*(4), 655–670. https://doi.org/10.5194/hess-6-655-2002

Al Bitar, A., Mialon, A., Kerr, Y. H., Cabot, F., Richaume, P., Jacquette, E., et al. (2017). The global SMOS Level 3 daily soil moisture and brightness temperature maps. *Earth System Science Data*, *9*(1), 293–315. https://doi.org/10.5194/essd-9-293-2017

Babaeian, E., Paheding, S., Siddique, N., Devabhaktuni, V. K., & Tuller, M. (2021). Estimation of root zone soil moisture from ground and remotely sensed soil information with multisensor data fusion and automated machine learning. *Remote Sensing of Environment*, *260*, 112434. https://doi.org/10.1016/j.rse.2021.112434

Babaeian, E., Sadeghi, M., Franz, T. E., Jones, S., & Tuller, M. (2018). Mapping soil moisture with the OPtical TRApezoid Model (OPTRAM) based on long-term MODIS observations. *Remote Sensing of Environment*, *211*, 425–440. https://doi.org/10.1016/j.rse.2018.04.029

Brocca, L., Moramarco, T., Melone, F., & Wagner, W. (2013). A new method for rainfall estimation through soil moisture observations. *Geophysical Research Letters*, *40*(5), 853–858. https://doi.org/10.1002/grl.50173

Brocca, L., Tarpanelli, A., Filippucci, P., Dorigo, W., Zaussinger, F., Gruber, A., & Fernández-Prieto, D. (2018). How much water is used for irrigation? A new approach exploiting coarse resolution satellite soil moisture products. *International Journal of Applied Earth Observation and Geoinformation*, *73*, 752–766. https://doi.org/10.1016/j.jag.2018.08.023

Chan, S. K., Bindlish, R., O'Neill, P. E., Njoku, E., Jackson, T., Colliander, A., et al. (2016). Assessment of the SMAP passive soil moisture product. *IEEE Transactions on Geoscience and Remote Sensing*, *54*(8), 4994–5007. https://doi.org/10.1109/tgrs.2016.2561938

Cook, M. J. (2014). *Atmospheric compensation for a landsat land surface temperature product*. Rochester Institute of Technology.

Cook, M. J., Schott, J. R., Mandel, J., & Raqueno, N. (2014). Development of an operational calibration methodology for the Landsat thermal data archive and initial testing of the atmospheric compensation component of a land surface temperature (LST) product from the archive. *Remote Sensing*, *6*(11), 11244–11266. https://doi.org/10.3390/rs61111244

Courault, D., Seguin, B., & Olioso, A. (2005). Review on estimation of evapotranspiration from remote sensing data: From empirical to numerical modeling approaches. *Irrigation and Drainage Systems*, *19*(3), 223–249. https://doi.org/10.1007/s10795-005-5186-0

Das, N. N., Entekhabi, D., Dunbar, R. S., Chaubell, M. J., Colliander, A., Yueh, S., et al. (2019). The SMAP and Copernicus Sentinel 1A/B microwave active-passive high-resolution surface soil moisture product. *Remote Sensing of Environment*, *233*, 111380. https://doi.org/10.1016/j.rse.2019.111380

Deines, J. M., Kendall, A. D., Butler, J. J., Basso, B., & Hyndman, D. W. (2021). Combining remote sensing and crop models to assess the sustainability of stakeholder-driven groundwater management in the U.S. high plains aquifer. *Water Resources Research*, *57*(3), e2020WR027756. https://doi.org/10.1029/2020wr027756

de Rosnay, P., Polcher, J., Laval, K., & Sabre, M. (2003). Integrated parameterization of irrigation in the land surface model ORCHIDEE. Validation over Indian Peninsula. *Geophysical Research Letters*, *30*(19), 1986. https://doi.org/10.1029/2003gl018024

FAO. (2021). *AQUASTAT—FAO's global information system on water and agriculture*. Food and Agriculture Organization of the United Nations (FAO). Website accessed on [2021/9/10].

Filippucci, P., Tarpanelli, A., Massari, C., Serafini, A., Strati, V., Alberi, M., et al. (2020). Soil moisture as a potential variable for tracking and quantifying irrigation: A case study with proximal gamma-ray spectroscopy data. *Advances in Water Resources*, *136*, 103502. https://doi.org/10.1016/j.advwatres.2019.103502

Foster, T., Brozović, N., & Butler, A. P. (2014). Modeling irrigation behavior in groundwater systems. *Water Resources Research*, *50*(8), 6370–6389. https://doi.org/10.1002/2014wr015620

Foster, T., Gonçalves, I. Z., Campos, I., Neale, C. M., & Brozović, N. (2019). Assessing landscape scale heterogeneity in irrigation water use with remote sensing and in situ monitoring. *Environmental Research Letters*, *14*(2), 024004. https://doi.org/10.1088/1748-9326/aaf2be

Foster, T., Mieno, T., & Brozović, N. (2020). Satellite-based monitoring of irrigation water use: Assessing measurement errors and their implications for agricultural water management policy. *Water Resources Research*, *56*(11), e2020WR028378. https://doi.org/10.1029/2020wr028378

Gettelman, A., Geer, A. J., Forbes, R. M., Carmichael, G. R., Feingold, G., Posselt, D. J., et al. (2022). The future of Earth system prediction: Advances in model-data fusion. *Science Advances*, *8*(14), eabn3488. https://doi.org/10.1126/sciadv.abn3488

Gibson, J., Franz, T. E., Wang, T., Gates, J., Grassini, P., Yang, H., & Eisenhauer, D. (2017). A case study of field-scale maize irrigation patterns in western Nebraska: Implications for water managers and recommendations for hyper-resolution land surface modeling. *Hydrology and Earth System Sciences*, *21*(2), 1051–1062. https://doi.org/10.5194/hess-21-1051-2017

Gibson, K. E., Gibson, J. P., & Grassini, P. (2019). Benchmarking irrigation water use in producer fields in the U.S. central Great Plains. *Environmental Research Letters*, *14*(5), 054009. https://doi.org/10.1088/1748-9326/ab17eb

Grant, R. F. (1995). Salinity, water use and yield of maize: Testing of the mathematical model *ecosys*. *Plant and Soil*, *172*(2), 309–322. https://doi.org/10.1007/bf00011333

Grant, R. F. (1997). Changes in soil organic matter under different tillage and rotation: Mathematical modeling in *ecosys*. *Soil Science Society of America Journal*, *61*(4), 1159–1175. https://doi.org/10.2136/sssaj1997.03615995006100040023x

Grant, R. F., Arkebauer, T. J., Dobermann, A., Hubbard, K. G., Schimelfenig, T. T., Suyker, A. E., et al. (2007). Net biome productivity of irrigated and rainfed maize-soybean rotations: Modeling versus measurements. *Agronomy Journal*, *99*(6), 1404–1423. https://doi.org/10.2134/agronj2006.0308

Grant, R. F., & Flanagan, L. B. (2007). Modeling stomatal and nonstomatal effects of water deficits on CO_2 fixation in a semiarid grassland. *Journal of Geophysical Research: Biogeosciences*, *112*(G3). https://doi.org/10.1029/2006jg000302

Grant, R. F., Jarvis, P. G., Massheder, J. M., Hale, S. E., Moncrieff, J. B., Rayment, M., et al. (2001). Controls on carbon and energy exchange by a black spruce-moss ecosystem: Testing the mathematical model *ecosys* with data from the BOREAS Experiment. *Global Biogeochemical Cycles*, *15*(1), 129–147. https://doi.org/10.1029/2000gb001306

Grant, R. F., Juma, N., Robertson, J., Izaurralde, R., & McGill, W. B. (2001). Long-term changes in soil carbon under different fertilizer, manure, and rotation: Testing the mathematical model *ecosys* with data from the Breton plots. *Soil Science Society of America Journal*, *65*(1), 205–214. https://doi.org/10.2136/sssaj2001.651205x

Grant, R. F., Kimball, B. A., Conley, M., White, J., Wall, G., & Ottman, M. J. (2011). Controlled warming effects on wheat growth and yield: Field measurements and modeling. *Agronomy Journal*, *103*(6), 1742–1754. https://doi.org/10.2134/agronj2011.0158

Grant, R. F., Kimball, B. A., Wall, G. W., Triggs, J. M., Brooks, T. J., Pinter, P. J., et al. (2004). Modeling elevated carbon dioxide effects on water relations, water use, and growth of irrigated Sorghum. *Agronomy Journal*, *96*(6), 1693–1705. https://doi.org/10.2134/agronj2004.1693

Grant, R. F., Lin, S., & Hernandez-Ramirez, G. (2020). Modeling nitrification inhibitor effects on N_2O emissions after fall- and spring-applied slurry by reducing nitrifier NH_4^+ oxidation rate. *Biogeosciences*, *17*(7), 2021–2039. https://doi.org/10.5194/bg-17-2021-2020

Grant, R. F., Rochette, P., & Desjardins, R. (1993). Energy exchange and water use efficiency of field crops: Validation of a simulation model. *Agronomy Journal*, *85*(4), 916–928. https://doi.org/10.2134/agronj1993.00021962008500040025x

Grant, R. F., Wall, G., Kimball, B., Frumau, K., Pinter, P. Jr., Hunsaker, D., & Lamorte, R. (1999). Crop water relations under different CO_2 and irrigation: Testing of *ecosys* with the free air CO_2 enrichment (FACE) experiment. *Agricultural and Forest Meteorology*, *95*(1), 27–51. https://doi.org/10.1016/s0168-1923(99)00017-9

Guan, K., Jin, Z., DeLucia, E. H., West, P., Peng, B., Tang, J., et al. (2022). A roadmap toward scalably quantifying field-level agricultural carbon outcome.

Haddeland, I., Lettenmaier, D. P., & Skaugen, T. (2006). Effects of irrigation on the water and energy balances of the Colorado and Mekong river basins. *Journal of Hydrology*, *324*(1), 210–223. https://doi.org/10.1016/j.jhydrol.2005.09.028

Hain, C. R., Crow, W. T., Anderson, M. C., & Yilmaz, M. T. (2015). Diagnosing neglected soil moisture source-sink processes via a thermal infrared-based two-source energy balance model. *Journal of Hydrometeorology*, *16*(3), 1070–1086. https://doi.org/10.1175/jhm-d-14-0017.1

Hurr, R. T., & Litke, D. W. (1989). Estimating pumping time and ground-water withdrawals using energy-consumption data. *Water-Resources Investigations Report*, *89*, 4107.

Irmak, S., Odhiambo, L. O., Kranz, W. L., & Eisenhauer, D. E. (2011). Irrigation efficiency and uniformity, and crop water use efficiency. *Biological Systems Engineering: Papers and Publications*, 451.

Jalilvand, E., Abolafia-Rosenzweig, R., Tajrishy, M., & Das, N. N. (2021). Evaluation of SMAP-Sentinel1 high-resolution soil moisture data to detect irrigation over agricultural domain. *IEEE Journal of Selected Topics in Applied Earth Observations and Remote Sensing*, *14*, 1–10747. https://doi.org/10.1109/jstars.2021.3119228

Jalilvand, E., Tajrishy, M., Hashemi, S. A. G. Z., & Brocca, L. (2019). Quantification of irrigation water using remote sensing of soil moisture in a semi-arid region. *Remote Sensing of Environment*, *231*, 111226. https://doi.org/10.1016/j.rse.2019.111226

Jiang, C., Guan, K., Pan, M., Ryu, Y., Peng, B., & Wang, S. (2020). BESS-STAIR: A framework to estimate daily, 30 m, and all-weather crop evapotranspiration using multi-source satellite data for the U.S. Corn Belt. *Hydrology and Earth System Sciences*, *24*(3), 1251–1273. https://doi.org/10.5194/hess-24-1251-2020

Jiang, C., Guan, K., Wu, G., Peng, B., & Wang, S. (2021). A daily, 250 m and real-time gross primary productivity product (2000–present) covering the contiguous United States. *Earth System Science Data*, *13*(2), 281–298. https://doi.org/10.5194/essd-13-281-2021

Jiang, C., & Ryu, Y. (2016). Multi-scale evaluation of global gross primary productivity and evapotranspiration products derived from Breathing Earth System Simulator (BESS). *Remote Sensing of Environment*, *186*, 528–547. https://doi.org/10.1016/j.rse.2016.08.030

Jiang, C., & Zhang, J. (2022). BESS-STAIR ET data set [Dataset]. Zenodo. https://doi.org/10.5281/zenodo.7251009

Jiang, L., Ma, E., & Deng, X. (2014). Impacts of irrigation on the heat fluxes and near-surface temperature in an inland irrigation area of Northern China. *Energies*, *7*(3), 1300–1317. https://doi.org/10.3390/en7031300

Keenan, T. F., Davidson, E., Moffat, A. M., Munger, W., & Richardson, A. D. (2012). Using model-data fusion to interpret past trends, and quantify uncertainties in future projections, of terrestrial ecosystem carbon cycling. *Global Change Biology*, *18*(8), 2555–2569. https://doi.org/10.1111/j.1365-2486.2012.02684.x

Kimm, H., Guan, K., Jiang, C., Peng, B., Gentry, L. F., Wilkin, S. C., et al. (2020). Deriving high-spatiotemporal-resolution leaf area index for agroecosystems in the U.S. Corn Belt using Planet Labs CubeSat and STAIR fusion data. *Remote Sensing of Environment*, *239*, 111615. https://doi.org/10.1016/j.rse.2019.111615

Koch, J., Zhang, W., Martinsen, G., He, X., & Stisen, S. (2020). Estimating net irrigation across the North China Plain through dual modeling of evapotranspiration. Water Resources Research, e2020WR027413.

Kumar, S. V., Peters-Lidard, C. D., Santanello, J. A., Reichle, R. H., Draper, C. S., Koster, R. D., et al. (2015). Evaluating the utility of satellite soil moisture retrievals over irrigated areas and the ability of land data assimilation methods to correct for unmodeled processes. *Hydrology and Earth System Sciences*, *19*(11), 4463–4478. https://doi.org/10.5194/hess-19-4463-2015

Lamb, S. E., Haacker, E. M. K., & Smidt, S. J. (2021). Influence of irrigation drivers using boosted regression trees: Kansas high plains. *Water Resources Research*, *57*(5), e2020WR028867. https://doi.org/10.1029/2020wr028867

Lawston, P. M., Santanello, J. A., Zaitchik, B. F., & Rodell, M. (2015). Impact of irrigation methods on land surface model spinup and initialization of WRF forecasts. *Journal of Hydrometeorology*, *16*(3), 1135–1154. https://doi.org/10.1175/jhm-d-14-0203.1

Lei, F., Crow, W. T., Kustas, W. P., Dong, J., Yang, Y., Knipper, K. R., et al. (2020). Data assimilation of high-resolution thermal and radar remote sensing retrievals for soil moisture monitoring in a drip-irrigated vineyard. *Remote Sensing of Environment*, *239*, 111622. https://doi.org/10.1016/j.rse.2019.111622

Li, K., Guan, K., Jiang, C., Wang, S., Peng, B., & Cai, Y. (2021). Evaluation of four new land surface temperature (LST) products in the U.S. Corn Belt: ECOSTRESS, GOES-R, Landsat, and Sentinel-3. *IEEE Journal of Selected Topics in Applied Earth Observations and Remote Sensing*, *14*, 1–9945. https://doi.org/10.1109/jstars.2021.3114613

Liu, Y., & Gupta, H. V. (2007). Uncertainty in hydrologic modeling: Toward an integrated data assimilation framework. *Water Resources Research*, *43*(7). https://doi.org/10.1029/2006wr005756

Luo, Y., Guan, K., & Peng, J. (2018). STAIR: A generic and fully-automated method to fuse multiple sources of optical satellite data to generate a high-resolution, daily and cloud-/gap-free surface reflectance product. *Remote Sensing of Environment*, *214*, 87–99. https://doi.org/10.1016/j.rse.2018.04.042

Luo, Y., Guan, K., Peng, J., Wang, S., & Huang, Y. (2020). STAIR 2.0: A generic and automatic algorithm to fuse Modis, Landsat, and Sentinel-2 to generate 10 m, daily, and cloud-/gap-free surface reflectance product. *Remote Sensing*, *12*(19), 3209. https://doi.org/10.3390/rs12193209

Malejane, D. N., Tinyani, P., Soundy, P., Sultanbawa, Y., & Sivakumar, D. (2018). Deficit irrigation improves phenolic content and antioxidant activity in leafy lettuce varieties. *Food Science & Nutrition*, *6*(2), 334–341. https://doi.org/10.1002/fsn3.559

Massari, C., Modanesi, S., Dari, J., Gruber, A., De Lannoy, G. J. M., Girotto, M., et al. (2021). A review of irrigation information retrievals from space and their utility for users. *Remote Sensing*, *13*(20), 4112. https://doi.org/10.3390/rs13204112

McCarthy, B., Anex, R., Wang, Y., Kendall, A. D., Anctil, A., Haacker, E. M. K., & Hyndman, D. W. (2020). Trends in water use, energy consumption, and carbon emissions from irrigation: Role of shifting technologies and energy sources. *Environmental Science & Technology*, *54*(23), 15329–15337. https://doi.org/10.1021/acs.est.0c02897

McDermid, S. S., Mahmood, R., Hayes, M. J., Bell, J. E., & Lieberman, Z. (2021). Minimizing trade-offs for sustainable irrigation. *Nature Geoscience*, *14*(10), 706–709. https://doi.org/10.1038/s41561-021-00830-0

Mezbahuddin, S., Spiess, D., Hildebrand, D., Kryzanowski, L., Itenfisu, D., Goddard, T., et al. (2020). Assessing effects of agronomic nitrogen management on crop nitrogen use and nitrogen losses in the Western Canadian prairies. *Frontiers in Sustainable Food Systems*, *4*, 512292. https://doi.org/10.3389/fsufs

Moradkhani, H. (2008). Hydrologic remote sensing and land surface data assimilation. *Sensors*, *8*(5), 2986–3004. https://doi.org/10.3390/s8052986

NASA. (2022). NLDAS-2 forcing data set [Dataset]. NASA LDAS (Land Data Assimilation System). https://ldas.gsfc.nasa.gov/nldas/v2/forcing

Nie, W., Kumar, S. V., Bindlish, R., Liu, P.-W., & Wang, S. (2022). Remote sensing-based vegetation and soil moisture constraints reduce irrigation estimation uncertainty. *Environmental Research Letters*, *17*(8), 084010. https://doi.org/10.1088/1748-9326/ac7ed8

Nie, W., Zaitchik, B. F., Rodell, M., Kumar, S. V., Anderson, M. C., & Hain, C. (2018). Groundwater withdrawals under drought: Reconciling GRACE and land surface models in the United States high plains aquifer. *Water Resources Research*, *54*(8), 5282–5299. https://doi.org/10.1029/2017wr022178

Ozdogan, M., Rodell, M., Beaudoing, H. K., & Toll, D. L. (2010). Simulating the effects of irrigation over the United States in a land surface model based on satellite-derived agricultural data. *Journal of Hydrometeorology*, *11*(1), 171–184. https://doi.org/10.1175/2009jhm1116.1

Pastorello, G., Trotta, C., Canfora, E., Chu, H., Christianson, D., Cheah, Y.-W., et al. (2020). The FLUXNET2015 data set and the ONEFlux processing pipeline for eddy covariance data. *Scientific Data*, *7*(1), 225.

Romaguera, M., Krol, M. S., Salama, M. S., Hoekstra, A. Y., & Su, Z. (2012). Determining irrigated areas and quantifying blue water use in Europe using remote sensing Meteosat Second Generation (MSG) products and Global Land Data Assimilation System (GLDAS) data. *Photogrammetric Engineering & Remote Sensing*, *78*(8), 861–873. https://doi.org/10.14358/pers.78.8.861

Romaguera, M., Krol, M. S., Salama, M. S., Su, Z., & Hoekstra, A. Y. (2014). Application of a remote sensing method for estimating monthly blue water evapotranspiration in irrigated agriculture. *Remote Sensing*, *6*(10), 10033–10050. https://doi.org/10.3390/rs61010033

Rosa, L., Chiarelli, D. D., Sangiorgio, M., Beltran-Peña, A. A., Rulli, M. C., D'Odorico, P., & Fung, I. (2020). Potential for sustainable irrigation expansion in a 3°C warmer climate. *Proceedings of the National Academy of Sciences*, *117*(47), 29526–29534. https://doi.org/10.1073/pnas.2017796117

Sadeghi, M., Babaeian, E., Tuller, M., & Jones, S. B. (2017). The optical trapezoid model: A novel approach to remote sensing of soil moisture applied to Sentinel-2 and Landsat-8 observations. *Remote Sensing of Environment*, *198*, 52–68. https://doi.org/10.1016/j.rse.2017.05.041

Scanlon, B. R., Faunt, C. C., Longuevergne, L., Reedy, R. C., Alley, W. M., McGuire, V. L., & McMahon, P. B. (2012). Groundwater depletion and sustainability of irrigation in the U.S. high plains and central valley. *Proceedings of the National Academy of Sciences*, *109*(24), 9320–9325. https://doi.org/10.1073/pnas.1200311109

Staff, S. S. (2022). Gridded Soil Survey Geographic (gSSURGO) database for Nebraska [Dataset]. United States Department of Agriculture, Natural Resources Conservation Service. https://data.nal.usda.gov/dataset/gridded-soil-survey-geographic-database-gssurgo

Stampoulis, D., Reager, J. T., David, C. H., Andreadis, K. M., Famiglietti, J. S., Farr, T. G., et al. (2019). Model-data fusion of hydrologic simulations and GRACE terrestrial water storage observations to estimate changes in water table depth. *Advances in Water Resources*, *128*, 13–27. https://doi.org/10.1016/j.advwatres.2019.04.004

Sun, L., Anderson, M. C., Gao, F., Hain, C., Alfieri, J. G., Sharifi, A., et al. (2017). Investigating water use over the Choptank River watershed using a multisatellite data fusion approach. *Water Resources Research*, *53*(7), 5298–5319. https://doi.org/10.1002/2017wr020700

Tang, J., & Grant, R. (2020). ECOSYS (version 1.0) [Software]. GitHub. https://github.com/jinyun1tang/ECOSYS

UNL. (2022). TAPS 2022 irrigation season comes to end amid drought. Website accessed on [2022/10.10].

U.S. GAO. (2019). *Irrigated agriculture: Technologies, practices, and implications for water scarcity*. United States Government Accountability Office.

USGS. (2018). *Water-use data available from USGS*. U.S. Geological Survey. Website accessed on [2021/10/1].

Van Dijk, A. I., Schellekens, J., Yebra, M., Beck, H. E., Renzullo, L. J., Weerts, A., & Donchyts, G. (2018). Global 5 km resolution estimates of secondary evaporation including irrigation through satellite data assimilation. *Hydrology and Earth System Sciences*, *22*(9), 4959–4980. https://doi.org/10.5194/hess-22-4959-2018

Vörösmarty, C. J., & Sahagian, D. (2000). Anthropogenic disturbance of the terrestrial water cycle. *BioScience*, *50*(9), 753–765. https://doi.org/10.1641/0006-3568(2000)050[0753:adottw]2.0.co;2

Wang, D., & Cai, X. (2007). Optimal estimation of irrigation schedule—An example of quantifying human interferences to hydrologic processes. *Advances in Water Resources*, *30*(8), 1844–1857. https://doi.org/10.1016/j.advwatres.2007.02.006

Wang, D., & Cai, X. (2009). Irrigation scheduling—Role of weather forecasting and farmers' behavior. *Journal of Water Resources Planning and Management*, *135*(5), 364–372. https://doi.org/10.1061/(asce)0733-9496(2009)135:5(364)

Wang, Y.-P., Trudinger, C. M., & Enting, I. G. (2009). A review of applications of model-data fusion to studies of terrestrial carbon fluxes at different scales. *Agricultural and Forest Meteorology*, *149*(11), 1829–1842. https://doi.org/10.1016/j.agrformet.2009.07.009

Weerts, A. H., & El Serafy, G. Y. (2006). Particle filtering and ensemble Kalman filtering for state updating with hydrological conceptual rainfall-runoff models. *Water Resources Research*, *42*(9). https://doi.org/10.1029/2005wr004093

Wei, S., Xu, T., Niu, G.-Y., & Zeng, R. (2022). Estimating irrigation water consumption using machine learning and remote sensing data in Kansas high plains. *Remote Sensing*, *14*(13), 3004. https://doi.org/10.3390/rs14133004

Wisser, D., Frolking, S., Douglas, E. M., Fekete, B. M., Vörösmarty, C. J., & Schumann, A. H. (2008). Global irrigation water demand: Variability and uncertainties arising from agricultural and climate data sets. *Geophysical Research Letters*, *35*(24), L24408. https://doi.org/10.1029/2008gl035296

Wright, R., Nunes, M. A., Lucey, P. G., Flynn, L., Ferrari-Wong, C., Gunapala, S., et al. (2020). HyTI: High spectral resolution thermal imaging from a 6U CubeSat. In *Paper presented at AGU Fall Meeting Abstracts*.

Wu, G., Guan, K., Jiang, C., Peng, B., Kimm, H., Chen, M., et al. (2020). Radiance-based NIRv as a proxy for GPP of corn and soybean. *Environmental Research Letters*, *15*(3), 034009. https://doi.org/10.1088/1748-9326/ab65cc

Xu, S., & Cheng, J. (2021). A new land surface temperature fusion strategy based on cumulative distribution function matching and multiresolution Kalman filtering. *Remote Sensing of Environment*, *254*, 112256. https://doi.org/10.1016/j.rse.2020.112256

Yang, Y., Guan, K., Peng, B., Pan, M., Jiang, C., & Franz, T. E. (2020). High-resolution spatially explicit land surface model calibration using field-scale satellite-based daily evapotranspiration product. *Journal of Hydrology*, *596*, 125730. https://doi.org/10.1016/j.jhydrol.2020.125730

Zappa, L., Schlaffer, S., Brocca, L., Vreugdenhil, M., Nendel, C., & Dorigo, W. (2022). How accurately can we retrieve irrigation timing and water amounts from (satellite) soil moisture? *International Journal of Applied Earth Observation and Geoinformation*, *113*, 102979. https://doi.org/10.1016/j.jag.2022.102979

Zaussinger, F., Dorigo, W., Gruber, A., Tarpanelli, A., Filippucci, P., & Brocca, L. (2019). Estimating irrigation water use over the contiguous United States by combining satellite and reanalysis soil moisture data. *Hydrology and Earth System Sciences*, *23*(2), 897–923. https://doi.org/10.5194/hess-23-897-2019

Zhang, C., & Long, D. (2021). Estimating spatially explicit irrigation water use based on remotely sensed evapotranspiration and modeled root zone soil moisture. *Water Resources Research*, *57*(12), e2021WR031382. https://doi.org/10.1029/2021wr031382

Zhang, J., Cai, X., Lei, X., Liu, P., & Wang, H. (2021). Real-time reservoir flood control operation enhanced by data assimilation. *Journal of Hydrology*, *598*, 126426. https://doi.org/10.1016/j.jhydrol.2021.126426

Zhang, J., Guan, K., Peng, B., Jiang, C., Zhou, W., Yang, Y., et al. (2021a). Challenges and opportunities in precision irrigation decision-support systems for center pivots. *Environmental Research Letters*, *16*(5), 053003. https://doi.org/10.1088/1748-9326/abe436

Zhang, J., Guan, K., Peng, B., Pan, M., Zhou, W., Grant, R. F., et al. (2021b). Assessing different plant-centric water stress metrics for irrigation efficacy using soil-plant-atmosphere-continuum simulation. *Water Resources Research*, *57*(9), e2021WR030211. https://doi.org/10.1029/2021wr030211

Zhang, J., Guan, K., Peng, B., Pan, M., Zhou, W., Jiang, C., et al. (2021c). Sustainable irrigation based on co-regulation of soil water supply and atmospheric evaporative demand. *Nature Communications*, *12*(1), 5549. https://doi.org/10.1038/s41467-021-25254-7

Zhang, K., Li, X., Zheng, D., Zhang, L., & Zhu, G. (2022). Estimation of global irrigation water use by the integration of multiple satellite observations. *Water Resources Research*, *58*(3), e2021WR030031. https://doi.org/10.1029/2021wr030031

Zhang, X., Zhou, J., Liang, S., & Wang, D. (2021). A practical reanalysis data and thermal infrared remote sensing data merging (RTM) method for reconstruction of a 1 km all-weather land surface temperature. *Remote Sensing of Environment*, *260*, 112437. https://doi.org/10.1016/j.rse.2021.112437

Zhou, W., Guan, K., Peng, B., Tang, J., Jin, Z., Jiang, C., et al. (2021). Quantifying carbon budget, crop yields, and their responses to environmental variability using the *ecosys* model for U.S. Midwestern agroecosystems. *Agricultural and Forest Meteorology*, *307*, 108521. https://doi.org/10.1016/j.agrformet.2021.108521